

UNIVERSITÀ
DEGLI STUDI
DI PADOVA



Model Predictive Control of HVAC Systems: Design and Implementation on a Real Case Study

Laureando
Giorgio Pattarello

Relatore
Prof. Ruggero Carli

Correlatore
Prof. Karl H. Johansson

Dipartimento di
Ingegneria
dell'Informazione

Anno 2013

Abstract

Recently, one of the most debated subjects regards energy savings. Since the percentage of the energy consumptions accounted for buildings is surprisingly higher than the one for the industries and transportations, the society is becoming more and more aware of the importance of the quality of building management. This gives an impulse to the automatic control community to design intelligent controllers for energy savings, a fact that appears evident also in the scientific literature. Many efforts have been spent in order to propose different control technique for the HVAC systems. However, only few papers deal with the implementation and test of the proposed controllers on a real case study. There is thus still the need of understanding what is critical in the implementation of such schemes, what affects the most the energy saving possibilities, and what is the critical and valuable information.

The final aim of this work is thus to design, implement and test a controller on a real testbed kindly provided by KTH Royal Institute of Technology. The control paradigm presented in this thesis is a model predictive controller that aims at saving energy as well as keeping the temperature and the carbon dioxide (CO₂) concentration in a comfort range that guarantees the wellness of room occupants. To improve the knowledge of the plant, we also study the problem of modeling both the dynamics of the system to be controlled and of the dedicated actuation system. Our experiments show that the obtained controller is able to satisfy the requests on energy savings and comfort, and hence can be used as a starting point for the design of efficient model based controllers of HVAC systems.

Acknowledgements

The path I walked on to get to where I am now has been very long and twisting but all the people I found along made my travel easier and enjoyable. From all of them I have learnt something that I will always carry with me. In this occasion I can write on paper how grateful I am to them.

First of all I would like to thank Prof. Ruggero Carli and Prof. Karl Henrik Johansson for having given me the opportunity to spend six beautiful months in Stockholm, learning, growing and enjoying. Without this experience probably I would not have been aware of some aspect of the life that sometimes after a while you may forget.

Thanks to Damiano, Alessandra, Marco and also Giulio for having been so patient, willing and kind with me in all the period I spent both inside and outside the department; in particular Damiano has been for me more than a supervisor and he helped me every time I had any kind of problem.

I want to thank also my parents and my sister. They always supported, trusted and believed in me in all the choices I have done in my life.

Thanks to Coba, Zano, Gamba, Guido and Michele for having been always real and honest friends. Especially I want to thank Coba and Marta for the big role they gave me in a very remarkable day of their life. I am very proud of this, and I am very proud of you all. I wish you all the best in your future because you deserve it.

Thanks to Valerio, Giulio, Demia and Alberto for making me feel in a family all the time. The time I spent with you was really great.

Thanks to all the HVAC group, especially Lin, Mani, Daniel, Ferran, Alireza, Afrooz and all the people who helped me and shared with me the technical problems of a real testbed; thanks also to Akademiska Hus for the support for the measurements.

Thanks to Andrea, Gianluca, Giacomo, Lorenza, Giulia M., Giulia V.,

Laura, Elena, all my past teammates and all the people with whom I shared also a little part of my life, because I will always have a little piece of you in me.

Thanks to Volpe and Lanza for having shared with me most of the troubles I have had to become an engineer.

I leave at the end a very special thanks for my grandparents. They have been like parents for me in all my life, they were always ready to help me and my family in every occasion they had. I owe you a lot.

Contents

1	Introduction	1
1.1	Contribution of the Thesis	2
1.2	Overview of the Thesis	3
2	HVAC systems	5
2.1	Description of general HVAC systems	5
2.2	Peculiarities of the KTH HVAC Testbed	13
3	Building model and System identification	29
3.1	Physics-based model	29
3.2	Devices to be identified	38
4	Control strategies	49
4.1	The current practice Proportional Integrative (PI) controller	49
4.2	The considered Model Predictive Control (MPC) strategy	51
5	Experimental Results	73
5.1	Testing the MPC solution adopted to control the cooling actuation	73
5.2	Test of the whole MPC	77
6	Conclusions	85
7	Further developments	87
	References	89

List of Figures

2.1	External view of the <i>Q building</i> in Stockholm, Sweden. The building is composed by 7 floors, from floor 2 to floor 8. Floor 2, that is actually the first floor, is underground.	13
2.2	Map of the second floor of the Q building. The floor is underground.	13
2.3	Diagram of the actuation systems present in the water tank lab. This scheme shows the degrees of freedom and the constraints that must be faced when designing air quality control schemes for the considered testbed.	15
2.4	Map showing the temperature of the water flowing through the radiators as a function of the external temperature. The map represents reference temperatures, since it neglects all the possible dynamics on these quantities.	16
2.5	Photos of one of the radiators, the fresh air inlet, the exhausted air outlet and the air conditioning outlet present in the water tank lab.	16
2.6	Scheme of the air inlets present in the water tank lab.	17
2.7	Scheme of the air conditioning system of the water tank lab. . .	18
2.8	SCADA interface of the system that provides the fresh air to the venting and cooling system	20
2.9	A Tmote Sky with highlighted the various measurements systems.	21
2.10	Typical star network topology, it is used also in our network . .	22
2.11	Map of the sensors deployed in the Kungliga Tekniska Hogskolan - Royal Institute of Technology (KTH) testbed	22
2.12	The people counting devices: left, the IRC3030 device. Right, the IRC3000.	24

2.13	A scheme representing the whole testbed system; LabVIEW is the tool that allow the user to communicate with the whole network by a collection of virtual instruments.	25
2.14	The web interface that allows every single user to download the sensed data and the actuation command of the system.	27
3.1	Electric scheme of the model of the walls. The three resistances $1/h_o$, R_{wall}^j and $1/h_i$ are placed between the equivalent temperature T_{ce}^j , and the temperatures $T_{\text{wall,o}}^j$, $T_{\text{wall,i}}^j$ and T_{room} . R_{wall}^j [$^{\circ}\text{C}/\text{W}$] and C^j [$\text{J}/^{\circ}\text{C}$] are the thermal resistance and the thermal capacity of the j-th wall respectively	32
3.2	Validation of the model performed with the software IDA ICE.	32
3.3	Comparison between the simulated temperatures obtained with the physical model and the actual measured room temperature.	33
3.4	Validation of the CO_2 physical model.	34
3.5	Fitting of the CO_2 models with the validation set of data.	36
3.6	Validation of the CO_2 models.	36
3.7	Picture of the motes attached to the radiator to run the test to get the mean radiant temperature.	39
3.8	Test on the radiators: first radiator temperature response. The motes are placed on the radiator in this order: 1032 on the top right, where there is the hot water inlet, 1035 on the top left, 1030 in the center, 1034 on the bottom left and 1033 on the bottom right, where there is the hot water outlet.	40
3.9	Test on the radiators: Comparison between motes in the first radiator (1035, 1030) and in the last (1036, 1037), placed in the same position on the radiator. Motes 1035 and 1036 are placed on the top left corner of the first and last radiator respectively, while Sensor 1030 and Sensor 1037 are placed in the center.	41
3.10	Relation between mass flow and opening valve percentage	44
3.11	Fitting between real supply air temperature of the air conditioning outlet and the simulated one.	46
4.1	Example of the actuation signals induced by the Akademiska Hus PI controller: cooling action.	50
4.2	Basic description of the main functioning of a Model Predictive Control (MPC) scheme [44].	54

5.1	Simulation on the second level MPC for the T_{sa} . The reference is set to 17°C the ventilation is constant at 30%.	74
5.2	Simulation on the second level MPC for the T_{sa} . The reference is set to 18°C the ventilation is constant at 30%.	74
5.3	Test on the equilibrium point method for the T_{sa} . The reference is set to 17°C and the ventilation is constant at 30%.	75
5.4	Test on the equilibrium point method for the T_{sa} . The reference is set to 18°C and the ventilation is constant at 30%.	75
5.5	Test on the MPC for the T_{sa} . The reference is set to 17°C and the ventilation is constant at 30%.	76
5.6	Test on the MPC for the T_{sa} . The reference is set to 18°C and the ventilation is constant at 30%.	76
5.7	Test 1 on the MPC. The temperature comfort bounds are set to 20 °C to 23 °C while the upper bound of the CO ₂ concentration is 700 ppm.	80
5.8	Test 2 on the MPC. The temperature comfort bounds are set to 20 °C to 23 °C while the upper bound of the CO ₂ concentration is 700 ppm.	81
5.9	Test 3 on the MPC. The temperature comfort bounds are set to 20 °C to 23 °C while the upper bound of the CO ₂ concentration is 700 ppm.	82
5.10	Test 4 on the MPC. The temperature comfort bounds are set to 20 °C to 23 °C while the upper bound of the CO ₂ concentration is 750 ppm.	83

1

Introduction

Buildings account for a surprisingly high percentage of energy consumption. As reported in [1], in 2004 the United States the management of buildings consumed the 41% of the total energy spent by mankind. In the EU this figure was reported to be 37% of the final energy, bigger than industry (28%) and transportation (32%) . In the UK, the proportion of energy use in building is 39%, slightly above the European average.

Environmental concerns pair with the large and attractive opportunities that exist to reduce buildings' energy use. To give some figures, the International Energy Agency's (IEA) targets a 77% reduction in the planet's carbon footprint by 2050. At the same time reports by the World Business Council for Sustainable Development (WBCSD) in 2009 suggest that the possibility of cutting the energy consumptions in buildings is dramatic, comparable to the amount of energy currently required by the entire transportation sector.

The vision of the mainstream researchers is that these energy savings can be achieved by exploiting information, or, to use a buzz-word, by implementing *intelligent buildings*. This means to control buildings using meaningfully the data coming from the various information sources available now or in the near future.

This trend of “smartening the buildings” is already a current trend of the next generation’s commercial buildings. For example, Building energy and comfort management (BECM) systems are control systems for individual buildings or groups of buildings that use computers and distributed micro-processors for monitoring, storing data and implementing communications between them. Since the average lifetime of a novel building ranges from 50 to 100 years, it is urgent to investigate how to build Heating, Venting and Air Conditioning (HVAC) systems in order to enhance their capabilities.

The role of the Automatic Controls community is then to understand:

- what are the limitations of the state-of-the art control schemes;
- how these limitations can be overcome by means of information.

More precisely, the aim is to understand what kind of information is needed to be energy efficient, and how to use it. For example, it might turn out that having accurate weather forecasts is much more important than having accurate buildings occupancy models, or that using MPC strategies does not lead to significant energy savings with respect to simpler strategies such as Proportional, Integrative and Derivatives (PIDs).

The current mainstream research is thus focusing on testing novel controllers and inferring what is critical from an information point of view.

1.1 Contribution of the Thesis

This thesis follows the current trend of considering Model Predictive Control (MPC) strategies. This control technique is popular mainly because of its capability to handle multivariate variable problems as well as to incorporate constraints for the manipulated and the controlled variables. It started being adopted in building climate control frameworks for also other reasons: the first is that the dynamics of buildings are usually slow, and this makes meaningful the fact of exploiting predictions. Moreover the comfort ranges, i.e., the aim of the control actions are precisely defined by European standards, helping thus the formalization process.

When applied to buildings, MPC schemes must face the peculiarity that building dynamics are highly affected by uncertainties. This implies that indoor climate predictive controllers must cope with disturbance rejection problems, the most being

- external weather conditions that do not follow exactly the forecasts provided by weather forecast systems;
- rooms occupancy patterns that are usually unknown or highly non stationary in time;
- sudden and unexpected changing conditions, like opening / closing windows or similar manual actions.

The role of this thesis is thus to analyze, standing on the shoulders of giants, what affects MPC schemes in real HVAC systems. Thus to see, from practical perspectives, what plays a critical role and what needs to be addressed in the future to improve their energy-savings performance.

Specifically the thesis describes in details the implementation of MPC schemes on a real testbed. By doing so we achieved some specific contributions, that can be summarized in:

- design and perform modeling and system identification of radiators and air ventilation systems. This with the aim of inferring the importance of having accurate actuators models;
- tailor classical MPC schemes to a real HVAC testbed, and identify the idealizations that are often assumed in literature. This aims to understand how much the practical problems encountered during implementations can lead to deviations from theoretical findings;
- perform comparisons with current practice controllers. This to have at least rough indications of what are the advantages of implementing advanced control schemes and what can actually be saved in terms of energy consumptions.

1.2 Overview of the Thesis

The manuscript is organized as follows. In Chapter 2 we review the literature related to the control of HVAC systems, introduce our case study and describe our testbed in details. In Chapter 3 instead we present the models of our system and the methodologies used to decipher the temporal behavior of the control-related variables. In Chapter 4 we illustrate the control strategy adopted, after

describing the general principles of MPC. In Chapter 5 we then picture the results obtained implementing the previously analyzed controllers. In the two final chapters 6 and 7, we eventually draw some conclusions and suggest some possible prospects for further developments and improvements.

2

HVAC systems

2.1 Description of general HVAC systems

An Heating, Venting and Air Conditioning (HVAC) system is a set of infrastructures, devices and actuators that are devoted to the conditioning of the air in buildings, i.e., to the control of the temperature, humidity and CO₂ levels.

This section presents a survey of the different technologies and methodologies present in literature and in practice. We remark that a big part of the literature is currently presenting simulative results that have actually never been tested on real testbeds. Thus there is currently a gap between the current practice and the theoretical studies performed by the various research groups.

General technologies used in HVAC systems

A common approach in the existing research projects on HVAC systems is to perform data acquisition and user activity detection exploiting Wireless Sensor Networks (WSNs). We notice that a general requirement is to use simple, wireless, binary sensors since they are cheap, easy to retrofit in existing buildings, require minimal maintenance and supervision, and do not require

users to change their behavior, e.g., have to be worn or carried. This means that doing research on HVAC systems requires to do not resort to any advanced sensing technology that is expensive, generating privacy concerns or requiring changes in user behavior, e.g., cameras, Radio Frequency Identification (RFID) tags, or wearable sensors.

In a schematic way, the most used hardware tools are:

- temperature, humidity, light and CO₂ sensors (wired, embedded on a mote or soldered on a wireless sensors boards);
- acoustic sensors (also microphones);
- Passive Infrared (PIR) sensors (for motion detection or people counting);
- switch-door sensors (magnetic);
- cameras;
- RFID tags.

Simple sensors are used in many energy intelligent buildings in the interest of activity recognition. For instance, PIR based sensors are often used (especially with lighting system) for occupancy detection. The sensors are connected directly to local lighting fixtures. These PIR sensors are also simple movement sensors and often cannot actually determine if the room is occupied or not. E.g., if the persons stand still, they will fail in detecting the occupancy. PIR sensors are used for instance in [2], where *Padmanabh et al.* investigate the joint use of microphones and PIR sensors for inferring the scheduling of conference rooms. An other project where PIR sensors have been used is the *AIM Project* [3], where authors used sensors to get some physical parameters, like temperature and light, as well as PIR to infer user presence in each room of a house.

Indoor activity recognition is in general implemented to provide inputs to a control strategy that aims for energy savings in buildings. To this aim, other sensors than PIRs can be used: in *Greener Building* [4] authors perform indoor activity recognition using simple infrared, pressure and acoustic sensors. An other strategy is to use door sensors. For instance [5] uses them in conjunction with PIR sensors to automatically turn off the HVAC system when the occupants are sleeping or away from home. Also in [6] *Agarwal et al.* chose to use a combination of a magnetic reed switch door sensor and a PIR sensor

module to build their building occupancy model. An even more complete testbed has been constructed in *ARIMA* [7]. Here, to gather data related to total building occupancy, wireless sensors are installed in a three-story building in eastern Ontario (Canada) comprising laboratories and 81 individual work spaces. Contact closure sensors are placed on various doors, PIR motion sensors are placed in the main corridor on each floor, and a carbon-dioxide sensor is positioned in a circulation area. In addition, the authors collect data on the number of people who log in to the network on each day. This thus gives possibility to the managers of the building to be aware of the air quality and to have CO₂ levels indications.

Other approaches are based on several simultaneous Sensor Networks. E.g., in [8] there are 3 independent complex sensor networks: one, Labview based, to acquire the indoor data (temperature at different height, humidity and CO₂), one to acquire the outdoor environmental data (temperature, humidity, lighting, acoustic and motion), and one to data log the system.

Information on the state of the considered system can of course be gathered also using measurement technology that directly infer the behavior of the occupants. An example is *iDorm* [9], where pressure pads are used to measure whether the user is sitting or lying on the bed as well as sitting on the desk chair. At the same time, a custom code that publishes the activity on the IP network senses computer-related activities of the user. The testbed thus measures several activities, like whether the occupant is running the computer's audio entertainment system or the video one. Other approaches are also to use entry-exit logs of the building security systems [10], or active badges, cameras, and vision algorithms. E.g., *Erickson et al.* propose a wireless network of cameras to determine real-time occupancy across a larger area in a building, [11, 12]. In [13] and [14], instead, the occupants should be equipped with sensor badges, with which it is possible to achieve relatively accurate localization using, for example, RFID tags.

Similarly, in *SPOTLIGHT* [15], the authors present a prototype system that can monitor energy consumption by individuals using a proximity sensor, while the building used in [16] is featured with an ultrasonic location system that is a 3D location system based on a principle of triangulation and relies on multiple ultrasonic receivers embedded in the ceiling and measures time-of-flight to them. The location system provides three-dimensional tracking solution.

In conclusion, in building energy and user comfort management area, WSNs

can play an important role by continuously and seamlessly monitoring the building energy use, which lays the foundation of energy efficiency in buildings. The sensor network provides basic tools for gathering the information on user behavior and its interaction with appliances from the home environment. Sensor Networks can also provide a mechanism for user identification, so that different profiles can be created for the different users living in the same apartment / house.

We finally remark that, in contrast with other smart home applications such as medical monitoring and security system, *applications focusing on energy conservation can tolerate a small loss in accuracy in favor of cost and ease of use*. Specially in building automation, occupants prefer to spend a little bit more but do not have to suffer to adapt to a new technology. Therefore, an energy intelligent building might not require cameras or wearable tags that may be considered intrusive to the user. Nevertheless, wireless sensor networks are today considered the most promising and flexible technologies for creating low-cost and easy-to-deploy sensor networks in scenarios like those considered by energy intelligent buildings.

General methodologies used in HVAC systems

There is an abundant literature on different approaches for the control of HVAC systems and for the treatment of the relative information.

Management of information on occupancy patterns as already said, one of the most influencing parameter in the management of HVAC systems is occupancy and occupant behavior.

Real-time occupancy is usually detected by means of inference techniques, where the information comes from sensor data [3, 4, 5, 6, 7, 2, 9]. It is in general also possible to exploit Bayesian inference techniques, usually with the aim of predicting the behaviors of the occupants.

In the *AIM* project [3], *Barbato et al.* build user profiles by using a learning algorithm that extracts characteristics from the user habits in the form of probability distributions. A sensor network continuously collects information about users presence/absence in each room of the house in a given monitoring period. At the end of this monitoring time the cross-correlation between each couple of 24 hour data presence patterns is computed for each room of the

house in order to cluster similar daily profiles.

In *OBSERVE* [11, 12], *Erickson et al.* construct a multivariate Gaussian model, a Markov Chain model, and an agent-based model for predicting user mobility patterns in buildings by using Gaussian and agent based models. The authors use a wireless cameras network for gathering traces of human mobility patterns in buildings. With this data and knowledge of the building floor plan, the authors create two prediction models for describing occupancy and movement behavior. The first model comprises of fitting a Multivariate Gaussian distribution to the sensed data and using it to predict mobility patterns for the environment in which the data is collected. The second model is an Agents Based Model (ABM) that can be used for simulating mobility patterns for developing HVAC control strategies for buildings that lack an occupancy sensing infrastructure. While the Markov Chain is used to model the temporal dynamics of the occupancy in a building.

In [17] authors propose a general method to predict the possible inhabitant service requests for each hour in energy consumption of a 24-hour anticipative time period. The idea is to exploit Bayesian networks to predict the user's behavior. In [18] authors adopt neural networks modeling the occupants behavior, and in cascade to this they create a system able to control temperature, light, ventilation and water heating.

Davidsson develops a Multi Agent System (MAS) for decision making under uncertainty for intelligent buildings, though this approach requires complex agents [13]. The system allocates one agent per room and the agents make use of pronouncers (centralized decision support), where decision trees and influence diagrams are used for decision-making purposes.

Similarly, the *iDorm* [9] learns and predicts the user's needs ability based on learning and adaptation techniques for embedded agents. Each embedded agent is connected to sensors and effectors, comprising a ubiquitous-computing environment. The agent uses a fuzzy-logic-based Incremental Synchronous Learning (ISL) system to learn and predict the user's needs, adjusting the agent controller automatically, non-intrusively, and invisibly on the basis of a wide set of parameters (which is one requirement for ambient intelligence).

In [19], authors propose a belief network for occupancy detection within buildings. The authors use multiple sensory input to probabilistically infer occupancy. By evaluating multiple sensory inputs, they determine the probability that a particular area is occupied. In each office, PIR and telephone on/off

hook sensors are used to determine if rooms are in occupied states. The authors use Markov chains to model the occupied state of individual rooms, where the transition matrix probabilities are calculated by examining the distribution of the sojourn times of the observed states.

All these works focus on the creation of occupancy models, that are then exploited for control purposes. There are indeed several manuscripts reporting usages of these models. E.g., in [20] daily occupancy profiles of occupancy are used in conjunction with a simple PID controller that works only on the heating accordingly to the profile, trying to set the indoor temperature to a certain set-point. In [5] the HVAC system is turned on or off when the occupants are away or asleep. This smart thermostat uses a Hidden Markov Chain (HMC) model to estimate the probability that the home is in one of the states *away*, *active* or *sleep* with transition every 5 minutes.

A lot of literature considers also model predictive control strategies applied to occupancy models. For example, in [8] *Dong et al.* use a Gaussian Mixture Model to categorize the changes of a selected feature. These are observations for an Hidden Markov Model that estimates the number of occupants. To estimate the duration of the occupants in a certain area it has been used a Semi Markov Model based on the pattern of the CO₂ acoustic, motion and lightning changes. All these information are given to a Non-Linear MPC that, solved by dynamic programming, gives the optimal control profile to use.

Management of weather forecasts predictions: we then notice that another big issue in smart HVAC control is how to manage predictions of weather forecasts. In general, predictive strategies (in the sense that account for weather predictions and their uncertainty) turn out to be more efficient and promising compared to the conventional, non predictive strategies in thermal control of buildings [21],[22],[23],[24],[25],[26].

In [24] authors have developed both certainty-equivalence controllers using weather predictions and a controller based on stochastic dynamic programming for a solar domestic hot water system. These strategies are based on probability distributions that are derived from available weather data. The simulation results show that these predictive control strategies can achieve lower energy consumptions compared to non-predictive strategies.

In [26] the use of a short-term weather predictor based on the real weather data in the control of active and passive building thermal storage inventory

is explored. The predicted variables include ambient air temperature, relative humidity, global solar radiation, and solar radiation. A receding horizon policy is applied, i.e., an optimization is computed over a finite planning horizon and only the first action is executed. At the next time step the optimization is repeated over a shifted prediction horizon. It has been shown that the electrical energy savings relative to conventional building control can be significant.

A predictive control strategy using a forecasting model of outdoor air temperature has been tailored in [23] to account for intermittently heated Radiant Floor Heating (RFH) systems. The control action here consists in deciding when to supply the heat to the floor. In the conventional intermittent control technique the decision is based on the past experience. The experimental results show that use of the predictive control strategy could save between 10% and 12% of the total energy consumption during the cold winter months compared to the existing conventional control strategy.

Other MPC techniques focus instead in the manipulation of passive thermal storage systems. E.g., [25] exploits predicted future disturbances while maintaining comfort bounds for the room temperature. Both conventional, non-predictive strategies and predictive control strategies are then assessed using a performance bound as a benchmark. To clarify, the performance bound is an ideal controller characterized by no mismatch between the controlled process model and the real plant and by perfectly known disturbances. As expected, predictive controllers may outperform the non-predictive ones and keep room temperatures within their comfort bounds with smaller energy requirements. Moreover in these cases low cost energy sources are exploited as much as possible. This project in fact considers both high-demand energy sources (e.g., chillers, gas boilers, conventional radiators) and low-demand energy methods (e.g., operation of blinds and evaporative cooling systems) for heating and cooling.

This is also the practice employed in standards 382/1 [27] and 380/4 [28] of Schweizerischer Ingenieurund Architektenverein (SIA 2). Low-demand energy sources make use of the thermal storage capacity of the building and thus are slow and heavily dependent on weather conditions. Hence the model predictive control should in this case fit very well: if predictions of the future system evolution can be computed, low cost energy sources can be used for controlling the building and meeting the occupants requirements. The aim is to avoid the conventional expensive energy sources as much as possible in favor of the low

cost ones.

In this context it is important to consider also the uncertainty of the predictions. [29, 30, 31, 32] have all considered also these uncertainties, even if in different ways. In [29], authors incorporate a stochastic occupancy model within the control loop. [30] instead proposes a stochastic predictive building temperature regulator where weather and load disturbances are modeled as Gaussian processes. [31] also uses a stochastic MPC and weather predictions. Firstly it solves a non-convex optimization problem and then it applies a disturbances feedback. [32] finally considers stochastic approach on the uncertainty of the forecast disturbances (the outside temperature, the occupancy and the solar radiation) solving the problem considering a scenarios based approach and a statistical learning procedure to learn these statistics from real and local data.

Effect of automatic blinds and lighting control also these systems have an important effect on heating and cooling requirements. A noticeable paper in this subject is [22], where the authors investigate the reduction in annual primary energy requirements for indoor climate control achieved in Rome by applying automated lighting control.

Remarks the current academic trend is to build testbeds and perform experiments on it to validate the simulative results. The most famous are the one from the *ETH Zurich* (Switzerland) [33], and the one of the *University of California, Berkeley*, [34]. Confirming a trend followed also in other automatic control frameworks, both these groups are applying Model Predictive Control strategies.

We nonetheless notice that the testbed considered in the current thesis has its own peculiarities, not only from topological points of view (i.e., the map of the building) but also in the structure of the HVAC system (i.e., the actuation system) and, even more importantly, in the climatic environment where it lies. Thus some care must be placed in comparing and assessing the architectural choices made by the designers of these testbeds.

2.2 Peculiarities of the KTH HVAC Testbed

Description of the system

The testbed lies in the same building of the KTH Automatic Control Laboratory in Stockholm, more precisely on the second floor of KTH *Q building*.



Figure 2.1: External view of the *Q building* in Stockholm, Sweden. The building is composed by 7 floors, from floor 2 to floor 8. Floor 2, that is actually the first floor, is underground.

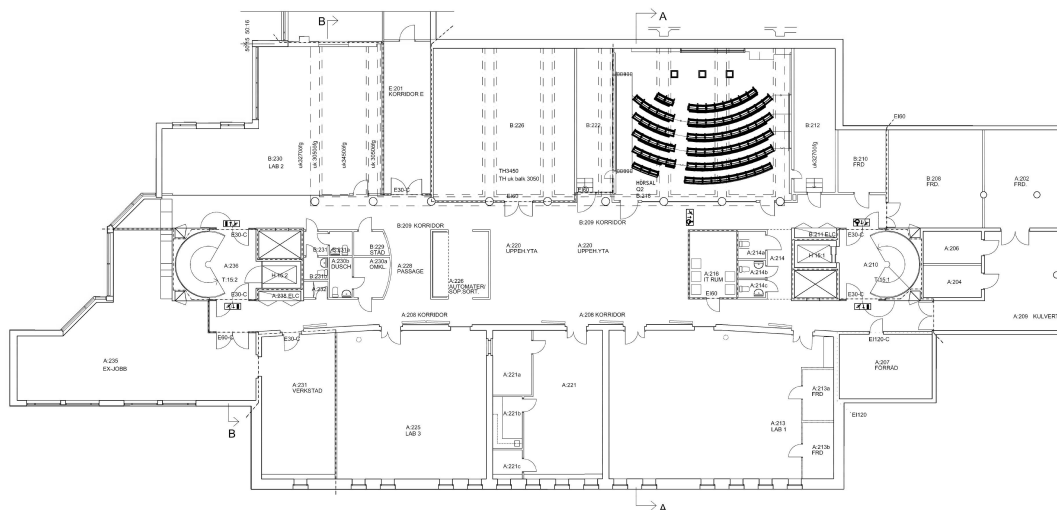


Figure 2.2: Map of the second floor of the *Q building*. The floor is underground.

The testbed comprises the floor shown in Figure 2.2. The floor is composed by a main corridor where all the rooms are facing: four laboratories, one

conference hall, one storage room and one study room. All the rooms of the second floor of the KTH Q building, except the storage room and a PCB Lab are equipped with a HDH sensor on the wall surface. This allows to detect temperature and CO₂ level in each rooms. Referring to Figure 2.2, the database gives information on the temperature and CO₂ of rooms A:213, A:225, A:235 and A:230. The thermal levels and the air quality of these rooms can then be controlled by venting, cooling and heating actuators.

Our attention is primarily on room A:225, informally called the *water tank lab*. In fact, due to regulations limitations, the research team performing automation experiments on this testbed has permissions to actuate only on this limited area of the second floor. To date, thus, this is the only room that is actively controlled.

The water tank lab (WTL) is equipped with:

- a WSN, that collects temperature, humidity, light and CO₂ values;
- a motion detection sensor;
- an occupancy sensor working as a people counter;
- an auxiliary PLC that allows the user to control the actuation signals.

We notice that the auxiliary PLC allows switching between the default controller (described in the following section 2.2) and the controllers implemented by the research team.

Since the final aim of the project is to control climate features of the indoor environment, it is of paramount importance to describe in precise details the functioning of the actuation systems. The main sources of climate control are 3: ventilation system, heating system and the cooling system. In the next sections we will describe them in precise details. For convenience we refer to the schematics offered in Figure 2.2.

Description of the air heating subsystem

The air heating system exploits common radiators. More precisely, in the WTL there are four radiators connected in parallel. As every normal radiator, they are heated by hot water transitioning through their circuits. It must be noticed that this heated water comes from a *district heating system*, also called

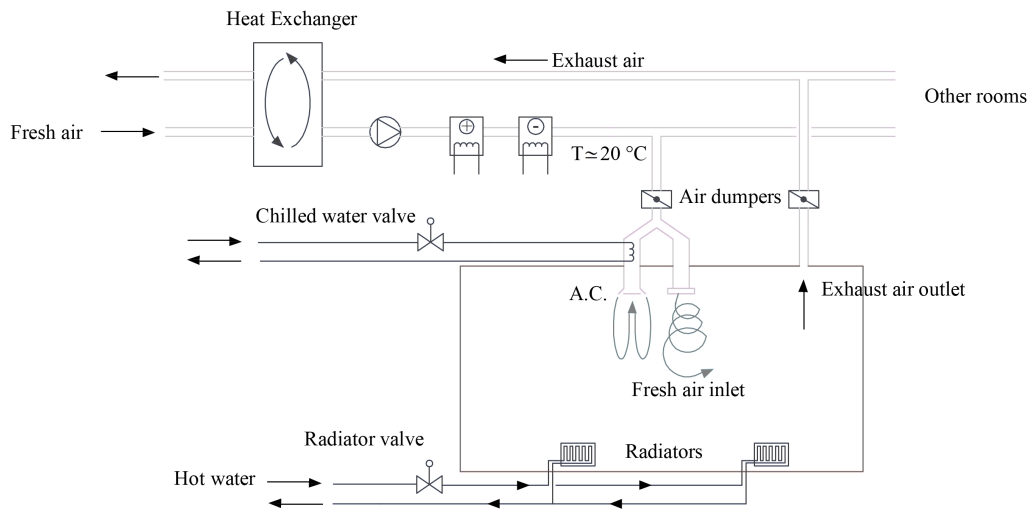


Figure 2.3: Diagram of the actuation systems present in the water tank lab. This scheme shows the degrees of freedom and the constraints that must be faced when designing air quality control schemes for the considered testbed.

*teleheating*¹. The hot water provided by the teleheating normally heats a secondary circuit. The water in the secondary circuit is then sent to the whole building with the aid of pumps and thus, eventually, to the WTL radiators.

This leads to the first important property of the testbed:

The temperature of the water flowing through the radiators is controlled by an external entity. The current controllers, on which the research team do not have authority, regulate this temperature using a static map taking as inputs the outside temperature conditions.

This map is shown in Figure 2.4.

What users can actively control is a valve placed before the first radiator and whose opening percentages can be set through a SCADA web-based interface. To help the development of controllers, the SCADA system accepts as inputs percentage values that are directly percentages of the total amount of the available heating power.

¹This kind of systems distribute heat generated in a centralized location to residential and commercial units. The heat is often obtained from cogeneration plants burning fossil fuels or biomasses (although heat-only boiler stations, geothermal heating and central solar heating are also used, as well as nuclear power). This generation mechanism is often used in Nordic countries, specially because it allows heating conversions far from the city walls but also because it uses both low quality heating sources and renewable energy sources.

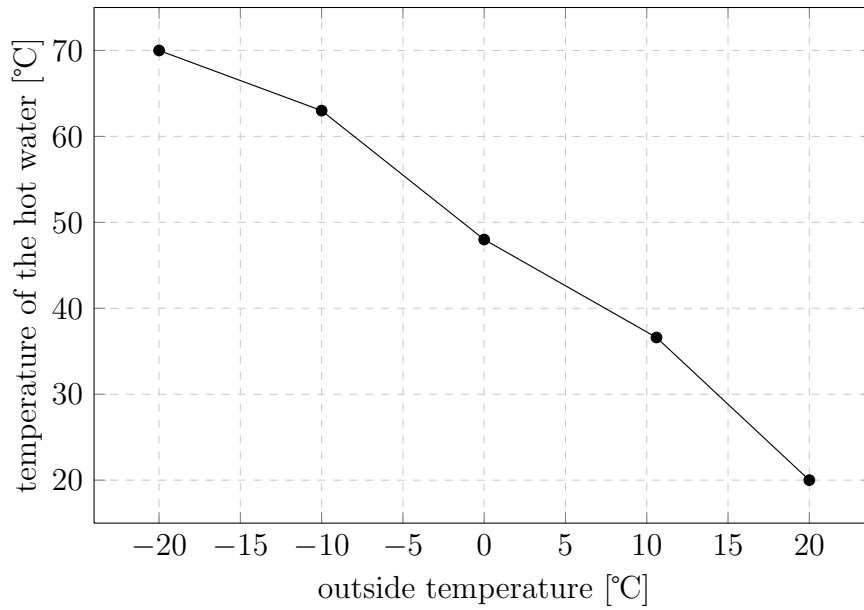


Figure 2.4: Map showing the temperature of the water flowing through the radiators as a function of the external temperature. The map represents reference temperatures, since it neglects all the possible dynamics on these quantities.

Description of the air venting and cooling subsystem

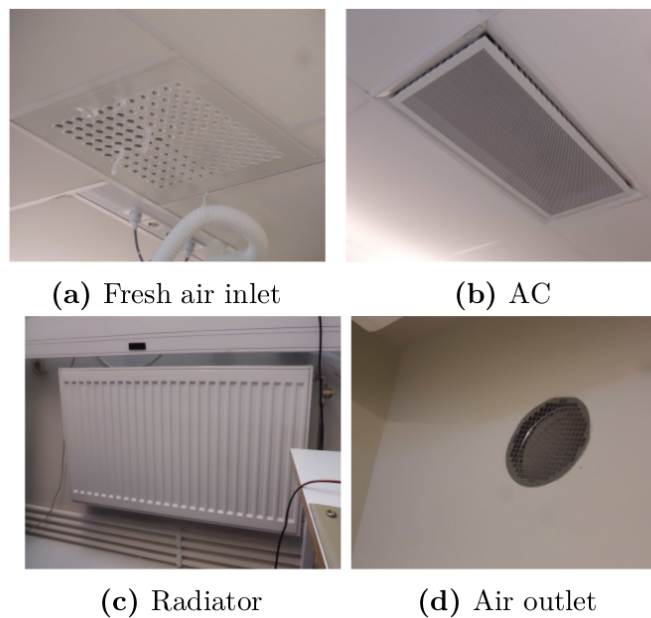


Figure 2.5: Photos of one of the radiators, the fresh air inlet, the exhausted air outlet and the air conditioning outlet present in the water tank lab.

In the Q building fresh air is supplied by means of three separated ventilation

units. The fresh air flow for areas with special applications (like laboratories or conference halls) is regulated by a Demand Controlled Ventilation (DCV), while for floors housing office areas there is instead a constant fresh air flow. In both these two cases venting is provided only in the day time and in a specific time slot, specifically from 07:00 to 16:00.

In our particular case the venting and the cooling systems are actually strictly connected. Indeed the air system comprises only one circuit that provides fresh air to the venting and cooling system at a temperature that is normally between 20 and 21 degrees, and that it is at the same pressure in the whole duct. In more details the system composed by heat exchanger, pumps and a heating/cooling system.

The ventilation system is composed by two parts: one for getting fresh air and one for taking away the exhausted air. Fresh air is supplied in the duct by one of the ventilation units, while the damper regulates the airflow that comes into the room. The air outlet is just a hole in the wall, where there is a tube with a dumper inside, that allows the air to flow through.

We notice that this exhaust air then flows into a duct that is eventually carried to the heater exchanger, so that a “free” pre-heating is performed to the fresh air coming inside. As shown in the schematics in Figure 2.6, in the WTL the ventilation duct is split in two equal branches, each with two ventilation and two air conditioning outputs.

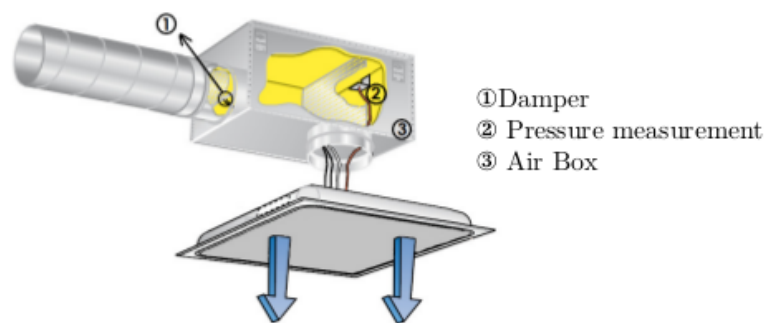


Figure 2.6: Scheme of the air inlets present in the water tank lab.

The cooling system is instead based on air conditioning units working with induction principles (a schematic drawing is shown in Figure 2.7). The primary

air, supplied by one of the ventilation units, is injected to a plenum². This plenum is equipped with nozzles of various sizes and small pipes from which the air can be discharged. Due to the high pressure in the plenum, the air comes out through the nozzles at a high velocity. This creates a zone with lower pressure, since an increase in the velocity produces a decrease of the pressure. This depression eventually causes the room air to be sucked up through a cooling heat exchanger, which consists of a coil where chilled water flows. In this way the air sucked from the room is cooled by this heat exchanger, then mixed with the primary air and eventually discharged into the room from the sides of the device.

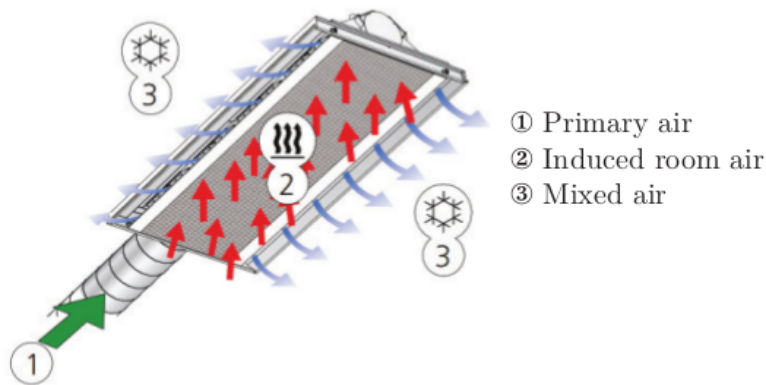


Figure 2.7: Scheme of the air conditioning system of the water tank lab.

We notice that the AC unit can also be used for heating purposes. In this case the only difference from the cooling process is that the water that is flowing in the coil is now warm. We notice that, as for the temperature of the water flowing through the radiators, the temperature of the water flowing through this cooling coil is not controllable by the users. As for the radiators case, also this temperature depends statically on the outside temperature. During our experiments this temperature was around 16 °C.

Continuing the analogy with the heating system, actuation of the cooling subsystem is performed through a valve that is placed before the chilled water circuit and whose opening percentage can be set using the SCADA web interface.

We notice that if the ventilation system is running only the venting subsystem, fresh air is coming from the cooling unit nozzles also (around the 30% of

²A plenum is a housing where it is created and stored air with a pressure greater than the atmospheric one

the total amount of the available air flow). Vice-versa, when we want to cool we need an air flow to chill. This leads us to notice the very important feature:

for the cooling system to be active we need the venting system to be active. This implies that once the cooling system is running the venting system is also running, and thus we must expect a air flow at around 20°C from the venting nozzles.

Effects of the ventilation on the cooling/heating as described before, the ventilation system affects both the heating and cooling processes. Figure 2.8 shows the entire air process in the schematic version that the user finds on the SCADA web interface. The previous processes can be summarized as follows:

1. the fresh air from outside is imported through a valve (denoted with the code ST201);
2. the air is then is filtered by opportune air filters;
3. after that the air is processed by an heater exchanger which exploits the heat of exhaust air flow. As shown in the Figure 2.8 the imported fresh air is warmed up to 19.4°C;
4. the pump TF001 then pushes the warmed air to the heating and cooling system sequentially; due to this the temperature of the fresh air that flows through the ducts is around 20°C in each room;
5. the fresh air is eventually discharged into the rooms at a temperature that is always around 20°C.

Summarizing, when the temperature of the room is below 20°C the air from the ventilation helps the heating system to increase the indoor temperature. Otherwise, if the temperature is greater then 20°Cthe ventilation system helps to lower the room temperature.

Soft PLCs and the default controller

For completeness we now describe what is the current practice.

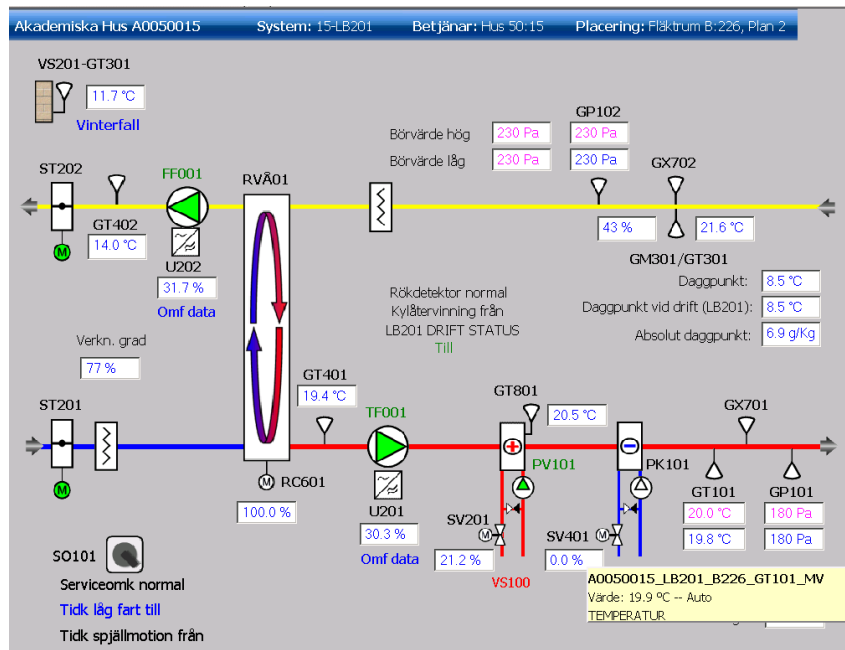


Figure 2.8: SCADA interface of the system that provides the fresh air to the venting and cooling system

In the Q building, the deployed ventilation units and cooling/heating processes are connected to three Soft PLCs³. One Soft PLC, placed on the second floor, manages the ventilation units and related sensors and actuators of the second and third floor. The other two PLCs are placed on the eighth floor, and control the corresponding devices of the fourth to eighth floor.

The Soft PLCs can be manually controlled over the SCADA system and their data saved on a server for post processing purposes. The default controllers, designed by Akademiska Hus, the Swedish agency running all the buildings of all the Swedish universities, are programmed to deliver a set-point temperature of 22 °C (with $\pm 1^\circ\text{C}$ dead band) and a CO₂ level below 850ppm. These thresholds are defined by the KTH Environmental and Building Department. More details can be found in Section 4.1 at page 49.

WSN

To gather further information on the status of the indoor environment the testbed features an ad-hoc Wireless Sensor Network (WSN) composed of *Tmote*

³A Soft PLC is basically a software package which emulates the functionality of a standard PLC inside a PC. The product that is used in the KTH testbed is a Fidelix Soft PLC. It has Internet access and is able to communicate as an OPC client to an OPC server.

Sky nodes. These *Tmote Sky* devices include a number of on-board sensors to measure light, temperature and humidity. In addition of that, other external sensors may be connected to the motes, using the dedicated ADC channel on the opportune expansion area.

In particular some motes are equipped with an additional CO₂ and temperature sensor (this has been done specially to avoid alterations in the measured temperatures induced by the heat that the motes microprocessor release, and also to reach places that could not be accessible in other ways).

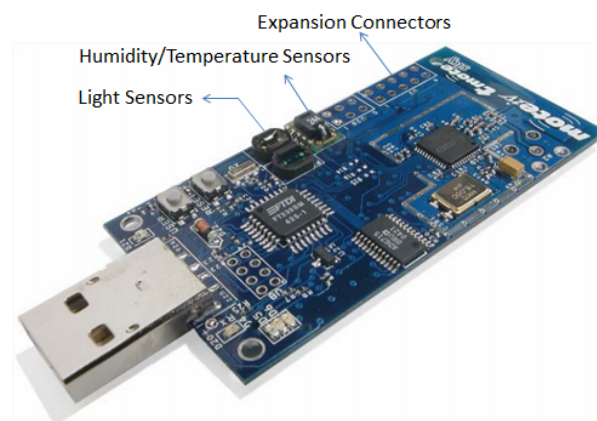


Figure 2.9: A Tmote Sky with highlighted the various measurements systems.

The WTL currently comprises 10 motes in the WTL, 4 motes in the rooms beside, 1 in the corridor and 1 outside the building. The nodes form a star network, and send data to a root mote directly connected with a server collecting and storing all the information (see Figure 2.11).

The motes forwards the sensed data to the main server every 30 seconds. The list of the nodes and of their main features are summarized in Table 2.1.

People counter

To measure the room occupancy the testbed features a tailored people counter, mounted over the entrance of the WTL. The counter is a thermal based camera commercialized by *IRISYS* and composed by two modules: the dual view IP and the node IP master.

The node IP master *IRC3000* [35] is a people counting devices with the imaging optics, sensor, signal processing and interfacing electronics all contained

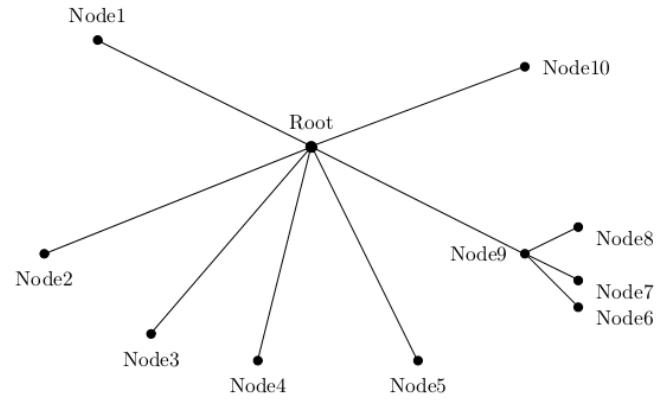


Figure 2.10: Typical star network topology, it is used also in our network

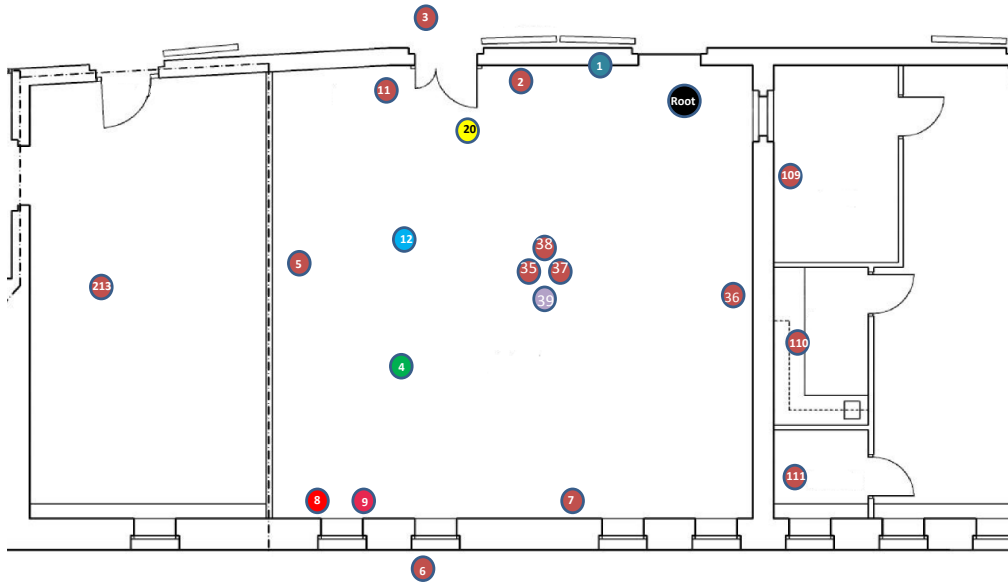


Figure 2.11: Map of the sensors deployed in the KTH testbed

Mote Id	Spot	T	H	C	L	Description
1000	WTL	-	-	-	-	Root
1001	WTL	✓	✓	✓	-	Exhaust air outlet
1002	WTL	✓	✓	-	-	Environment
1003	Corridor	✓	✓	-	-	Corridor
1004	WTL	✓	✓	✓	-	Fresh air inlet
1005	WTL	✓	✓	-	-	Room wall temperature
1006	Outside	✓	✓	-	-	Outdoor wall temperature
1007	WTL	✓	✓	-	-	Room wall temperature
1008	WTL	✓	-	-	-	Surface of radiator hot water inlet
1009	WTL	✓	-	-	-	Surface of radiator hot water outlet
1011	WTL	✓	✓	-	-	Room wall temperature
1012	WTL	✓	✓	-	-	Air conditioning outlet
1020	WTL	-	-	-	✓	Environment
1035	WTL	✓	✓	-	-	Environment
1036	WTL	✓	✓	-	-	Room wall temperature
1037	WTL	✓	✓	-	-	Ceiling
1038	WTL	✓	✓	-	-	Floor
1039	3rd Floor	✓	✓	-	-	Floor
1109	PCB Lab	✓	✓	-	-	Beside room environment
1110	PCB Lab	✓	✓	-	-	Beside room environment
1111	PCB Lab	✓	✓	-	-	Beside room environment
1213	Storage room	✓	✓	-	-	Beside room environment

Table 2.1: Summary of the mote of the WSN (T, H, C, L stand for temperature, humidity, CO₂ and light respectively)

within a molded plastic housing. The unit is used in a downward looking manner, as the unit functions optically recognize the heat emitted by people passing underneath as infrared radiation, collected through a germanium lens with a 60' field of view. The sensing area is a square on the floor whose width is approximately equal to the mounting height.

The dual view IP *IRC3030* [36] multiplexes both the thermal people count data, the stored count data, diagnostic information and the video stream into a single IP data stream. The IP capability allows remote viewing, configuration and data collection over IP infrastructure, either over an in-store LAN, or for worldwide viewing from remote locations over the Internet.

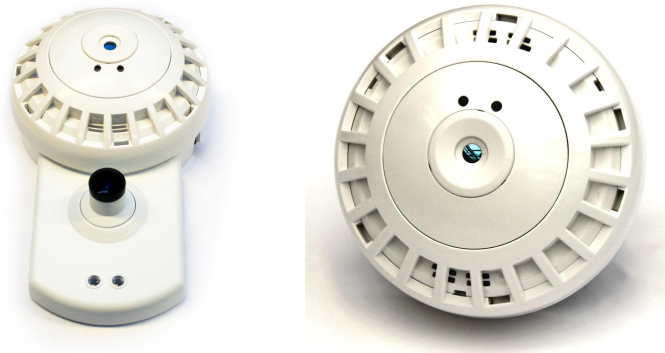


Figure 2.12: The people counting devices: left, the IRC3030 device. Right, the IRC3000.

Programmable Logic Controller (PLC)

In addition to the soft PLC the testbed comprises an additional PLC, a *Fidelix FX-2025A* [37], that allows to communicate and actuate. The device is endowed with a freely programmable web server, based on an industrial PC running a Windows CE operating system. The device accesses to all the data of the Akademiska Hus central system and can send command to the actuation devices. Moreover it is also connected to the dedicated temperature, CO₂ and binary motion sensors present in the testbed.

Weather forecasts

As highlighted in our literature review, the knowledge of the future outdoor conditions is crucial for achieving good control performance in terms of energy savings. To this aim the testbed server fetches and stores information the web site www.wunderground.com. More precisely, the available data are:

- temperature (current and the hourly forecasts for the next 72 hours);
- wind speed (current and the hourly forecasts for the next 72 hours);
- wind direction (current and the hourly forecasts for the next 72 hours);
- wind gusts (only the current status);
- precipitation (current and the hourly forecasts for the next 72 hours);
- external air pressure (only the current status).

Central PC and LabVIEW

The pulsing heart of the testbed is located in a dedicated server running in the WTL. This server implements all the logic that allows the user to perform all the possible communications with the various devices. The instruments that make these communications possible have been designed and developed in LabVIEW. The server is connected through Ethernet cables to the KTH network and to the external PLC, and is reachable through dedicated TCP-IP Internet ports. A schematic representation of the whole communication system is shown in Figure 2.13.

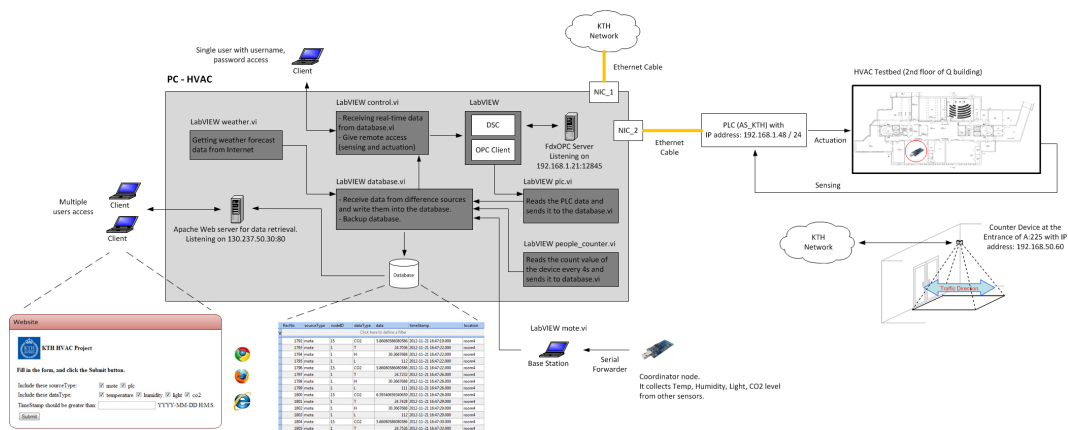


Figure 2.13: A scheme representing the whole testbed system; LabVIEW is the tool that allow the user to communicate with the whole network by a collection of virtual instruments.

PLC virtual instrument the server continuously runs an OPC Server that listens data coming from the dedicated PLC. In the meantime, an OPC Client runs on a virtual instrument and processes this data from the PLC. Eventually, this information is sent to the dedicated database.

People counter and weather virtual instruments the information coming from the people counter is processed by a dedicated virtual instrument, `people_counter.vi`, that reads the counted value of the device every four seconds and sends it to the virtual instrument managing the database. A similar procedure is implemented to manage the weather forecasts, `weather.vi`.

Motes virtual instrument the root of the dedicated WSN is mounted on one of the USB ports of the server. Through a serial forwarding, the data from this root wireless node are then processed by a dedicated virtual instrument, `mote.vi`, that sends in turn these data to the database virtual instrument.

Database and control virtual instruments all the data coming from the previous virtual instruments are received by an additional virtual instrument, `database.vi`, that writes them into a database. This instrument sends also these real-time data to another virtual instrument, `control.vi`, that enables users to have remote access to the sensed data and it also allows the actuation. We notice that user can have access to this information only through an appropriate client and credentials.

Remote access

As already written in the previous sections, all the sensed information is stored into a database. The central server also runs an *Apache Web Server* that allows the access to this database through the dedicated web page `http://hvac.ee.kth.se/`. With a simple web interface, shown in Figure 2.14, it is possible to download information about the system in a handy `.txt` file.

Accessing the data and giving actuation commands is possible by using some other virtual instruments, like `ControlConnectToHVAC.vi` or `ControlGetDataPlcs.vi`⁴. These instruments thus allow every user with LabVIEW to potentially actuate remotely the system. Some of these instruments have also been implemented in *Matlab*, so that users can run control algorithms remotely.

⁴The complete list can be found on https://code.google.com/p/kth-hvac/wiki/RemoteAccess#Creating_connection_to_HVAC_system with more explanations on how to use them, and also with the possibility of downloading them.

Step 1. Select the data you want:

<input type="checkbox"/> Indoor Environment	<input type="checkbox"/> Outdoor Environment	<input type="checkbox"/> Actuation Values	<input type="checkbox"/> Weather Forecast
<input type="checkbox"/> Temperature (°C)	<input type="checkbox"/> Temperature (°C)	<input type="checkbox"/> Fresh air inlet valve opening (%)	<input type="checkbox"/> Temperature (°C)
<input type="checkbox"/> Humidity (RH%)	<input type="checkbox"/> Humidity (RH%)	<input type="checkbox"/> Exhaust air outlet valve opening (%)	<input type="checkbox"/> Wind Speed (Kph)
<input type="checkbox"/> CO ₂ (ppm)		<input type="checkbox"/> AC valve opening (%)	<input type="checkbox"/> Wind Direction (degree)
<input type="checkbox"/> Light (lux)		<input type="checkbox"/> Radiator valve opening (%)	<input type="checkbox"/> Wind Gusts (Kph)
<input type="checkbox"/> Pressure (Pa)			<input type="checkbox"/> Precipitation (mm)
<input type="checkbox"/> Pump opening (%)			<input type="checkbox"/> External Air Pressure (mBar)
<input type="checkbox"/> Binary Motion			
<input type="checkbox"/> Occupancy			
<input type="checkbox"/> Events ¹			

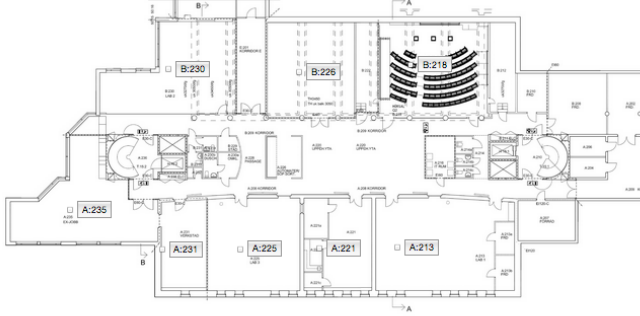
Weather forecast range:
+0 Hour

Step 2. Select the time interval:

From²: 13-06-18 00:00:00 Today

To³: 13-06-18 23:59:59 Today

Step 3. Select the locations:



Submit

Figure 2.14: The web interface that allows every single user to download the sensed data and the actuation command of the system.

3

Building model and System identification

3.1 Physics-based model

Model based control paradigms need a mathematical description of the system of interest. For this reason, in this chapter we shall deal with the derivation of a proper model which accurately describes the dynamics of the signals involved in the system. In particular, aiming at controlling the comfort features, we are interested in the behaviour of two physical characteristics, which are the temperature of the room and the concentration of CO₂. In this work, we shall not focus on humidity, due to the fact that in the testbed there is no device capable of modifying its evolution (i.e. there is no dehumidifier or similar devices). In order to describe the mentioned quantities, we adopted a physical modeling of the whole system (white-box approach), using as reference [32]. In such work, authors derive models that try to explain the system using relatively simple relations, still keeping a good degree of accuracy (i.e. such that the system is well described). In this way, the computational burden of the model remains low, according to the needs of MPC controllers. These models are

built under the following assumptions:

- no infiltrations are considered, so that the inlet airflow in the zone equals the outlet airflow;
- the zone is well mixed, i.e. the temperature and the concentration of CO₂ are constant with respect to the space and do not depend on the place they are measured;
- the thermal effects of the vapor production are neglected.

All the parameters involved in this subsection are described in Table 3.1

Room temperature model

As in [32], the room temperature is computed via the following energy balance of the zone, modeled as a lumped node.

$$m_{\text{air,zone}} c_{\text{pa}} \frac{dT_{\text{room}}}{dt} = Q_{\text{vent}} + Q_{\text{cool}} + Q_{\text{heat}} + Q_{\text{int}} + \sum_j Q_{\text{wall},j} + \sum_j Q_{\text{win},j}. \quad (3.1)$$

In (3.1), the left-hand term represents the heat stored in the air within the room. Q_{vent} is the heat flow due to ventilation, Q_{cool} and Q_{heat} are the heating and cooling flows. These are necessary in order to keep the room environment within thermally comfortable conditions. The quantity Q_{int} incorporates the internal gains, which are given by the sum of the heat flows due to occupancy, equipment and lighting. $Q_{\text{wall},j}$ and $Q_{\text{win},j}$ represent the heat flows exchanged between walls and room and windows and room respectively. Each term of the Equation (3.1) is:

$$\begin{aligned} Q_{\text{vent}} &= \dot{m}_{\text{vent}} c_{\text{pa}} \Delta T_{\text{vent}} = \dot{m}_{\text{vent}} c_{\text{pa}} (T_{\text{ai}} - T_{\text{room}}), \\ Q_{\text{cool}} &= \dot{m}_{\text{cool}} c_{\text{pa}} \Delta T_{\text{cool}} = \dot{m}_{\text{cool}} c_{\text{pa}} (T_{\text{sa}} - T_{\text{room}}), \\ Q_{\text{heat}} &= A_{\text{rad}} h_{\text{rad}} \Delta T_{\text{rad}} = A_{\text{rad}} h_{\text{rad}} (T_{\text{mr}} - T_{\text{room}}), \\ Q_{\text{int}} &= c N_{\text{people}}, \\ Q_{\text{wall},j} &= h_i A_{\text{wall}}^j (T_{\text{wall},i}^j - T_{\text{room}}), \\ Q_{\text{win},j} &= \frac{(T_{\text{amb}} - T_{\text{room}})}{R_{\text{win}}^j} + G^j A_{\text{win}}^j I^j. \end{aligned} \quad (3.2)$$

From (3.1) and (3.2) we obtain the differential equation

$$\begin{aligned}
\frac{dT_{\text{room}}}{dt} = & \frac{\dot{m}_{\text{vent}}(T_{\text{ai}} - T_{\text{room}})}{m_{\text{air,zone}}} + \frac{\dot{m}_{\text{cool}}(T_{\text{sa}} - T_{\text{room}})}{m_{\text{air,zone}}} + \frac{A_{\text{rad}}h_{\text{rad}}(T_{\text{mr}} - T_{\text{room}})}{m_{\text{air,zone}}c_{\text{pa}}} \\
& + \frac{cN_{\text{people}}}{m_{\text{air,zone}}c_{\text{pa}}} + \sum_j \frac{h_i A_{\text{wall}}^j (T_{\text{wall,i}}^j - T_{\text{room}})}{m_{\text{air,zone}}c_{\text{pa}}} \\
& + \sum_j \frac{(T_{\text{amb}} - T_{\text{room}})}{R_{\text{win}}^j m_{\text{air,zone}}c_{\text{pa}}} + \frac{\sum_j G^j A_{\text{win}}^j I^j}{m_{\text{air,zone}}c_{\text{pa}}}
\end{aligned} \tag{3.3}$$

In order to have the whole description of the temperature dynamics, we also need to model the behavior of the indoor wall temperature, say $T_{\text{wall,i}}^j$, of each surface. These temperature signals are calculated by means of an energy balance between the outdoor and indoor surfaces. All the walls are modeled as a “two capacitance and three resistance” systems (2C3R), where the thermal capacity, denoted by C^j , is determined using the Active Heat Capacity model proposed by [38]. A representation of such a model is shown in Figure 3.1; solving the circuit we can find in/out relationships for wall temperatures. More precisely, such relationships are

$$\frac{dT_{\text{wall,o}}^j}{dt} = \frac{\left[h_o A_{\text{wall}}^j (T_{\text{ee}}^j - T_{\text{wall,o}}^j) + \frac{(T_{\text{wall,i}}^j - T_{\text{wall,o}}^j)}{R_{\text{wall}}^j} \right]}{C^j/2} \tag{3.4}$$

$$\frac{dT_{\text{wall,i}}^j}{dt} = \frac{\left[h_i A_{\text{wall}}^j (T_{\text{room}} - T_{\text{wall,i}}^j) + \frac{(T_{\text{wall,o}}^j - T_{\text{wall,i}}^j)}{R_{\text{wall}}^j} \right]}{C^j/2} \tag{3.5}$$

The equivalent external temperature T_{ee}^j accounts for the different radiation heat exchange due to the orientation of the external walls. The outdoor temperature is modified by the effects of radiation on the j -th wall.

$$T_{\text{ee},j} = T_{\text{amb}} + \frac{aI^j}{\alpha_e}. \tag{3.6}$$

All the values of the parameters were determined by means of evaluations based on the geometry of the building, the manufacturing materials and the knowledge

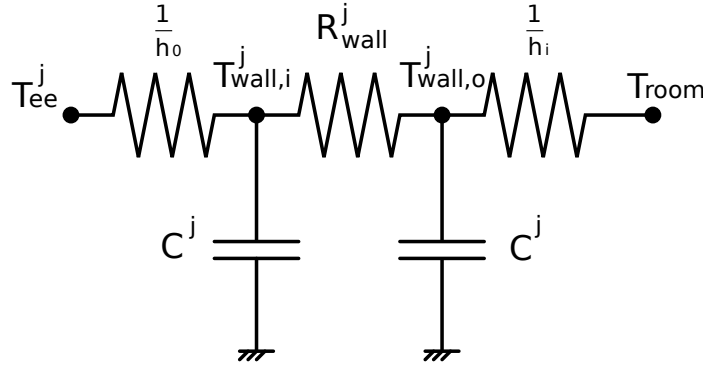


Figure 3.1: Electric scheme of the model of the walls. The three resistances $1/h_o$, R_{wall}^j and $1/h_i$ are placed between the equivalent temperature T_{ee}^j , and the temperatures $T_{wall,o}^j$, $T_{wall,i}^j$ and T_{room} . R_{wall}^j [$^{\circ}\text{C}/\text{W}$] and C^j [$\text{J}/^{\circ}\text{C}$] are the thermal resistance and the thermal capacity of the j -th wall respectively

of the construction standards. The resulting model was validated to be in accordance with the Stockholm climate. Its outcomes were compared with the predicted values given by simulations carried out in IDA [39], which represents one of the most effective softwares for building model simulations. The data regarding the climate conditions were taken from the Swedish Meteorological and Hydrological Institute (SMHI). The comparison was performed under the same conditions of ventilation, solar radiation, internal gains and occupancy. In both cases, thermal bridges and infiltrations were neglected. In order to clearly display the effects of the thermal behavior of the room model, no heating and cooling systems were simulated. The results are depicted in Figure 3.10.

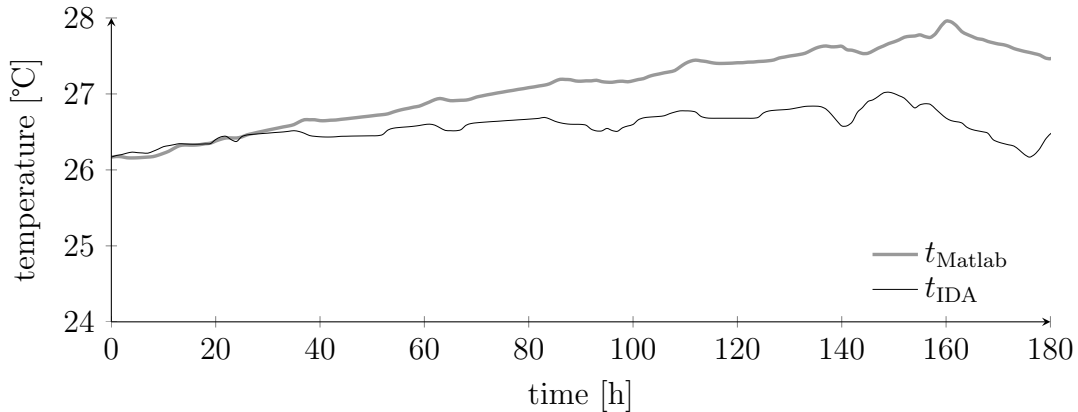


Figure 3.2: Validation of the model performed with the software IDA ICE.

In Figure 3.3 a comparison between the simulation of the model using real

inputs and the measured temperature of the room is shown. Unfortunately, it

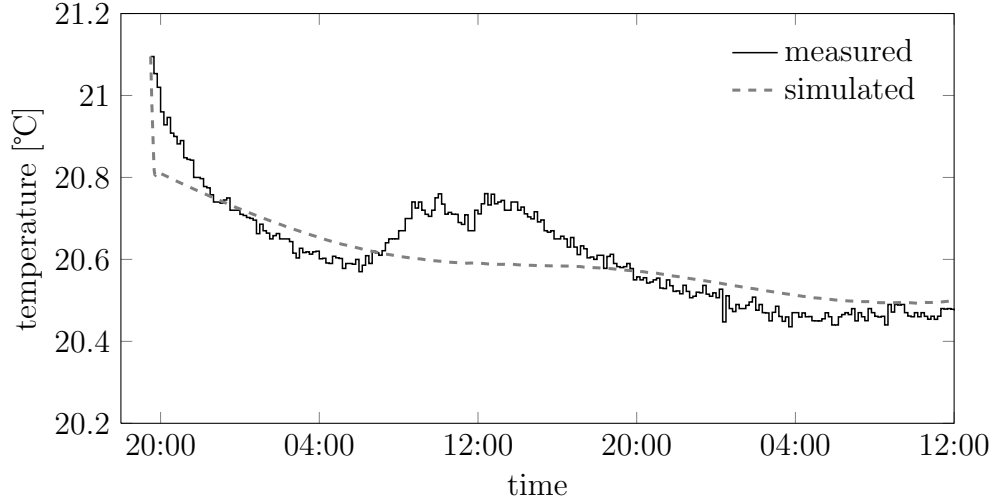


Figure 3.3: Comparison between the simulated temperatures obtained with the physical model and the actual measured room temperature.

appears that the model is not able to fit adequately with the measured data. However, it may be good for capturing long period trends. The faster dynamics of the room temperature are not properly followed by our model. Nevertheless, we shall make use of this model, since we assessed that its accuracy is good enough for our purposes.

CO₂ concentration model

As in [32], the CO₂ concentration model is determined by a balance between the amount of CO₂ that is flowing inside the room C_{in} , the amount flowing outside¹ because of the air outlet pump C_{out} , and the amount of CO₂ that is generated by the occupants C_{occ} . More precisely, assuming no leakages, i.e. no spontaneous outflowing of air, this balance leads to

$$V \frac{dC_{CO_2}}{dt} = C_{in} - C_{out} + C_{occ}. \quad (3.7)$$

where

¹We made the reasonable assumption that the air flowing out of the room has the same concentration CO₂ of the air inside the room

$$\begin{aligned}
C_{\text{in}} &= \dot{m}_{\text{air}} C_{\text{CO}_2, \text{i}}, \\
C_{\text{out}} &= \dot{m}_{\text{air}} C_{\text{CO}_2}, \\
C_{\text{occ}} &= g_{\text{CO}_2} N_{\text{people}},
\end{aligned} \tag{3.8}$$

From (3.7) and (3.8) we obtain the differential equation

$$\frac{dC_{\text{CO}_2}}{dt} = \frac{\dot{m}_{\text{air}} C_{\text{CO}_2, \text{i}}}{V} - \frac{\dot{m}_{\text{air}} C_{\text{CO}_2}}{V} + \frac{g_{\text{CO}_2} N_{\text{people}}}{V}. \tag{3.9}$$

The derived model was then discretized by using the Euler backward method, which yields (the sampling time is neglected for simplicity)

$$C_{\text{CO}_2}(t+1) = C_{\text{CO}_2}(t) + \dot{m}_{\text{air}}(C_{\text{CO}_2}(t) - C_{\text{CO}_2, \text{i}}) + g_{\text{CO}_2} N_{\text{people}}(t). \tag{3.10}$$

We assessed that this model could not describe the CO_2 behaviour accurately enough. Its main drawback is given by the fact that no zero decaying happens if the system is not excited. In this way, all the unavoidable errors accumulate, making the model outcomes differ substantially from the real behavior. An example of this is in Figure 3.4. For this reason, we decided to identify a new

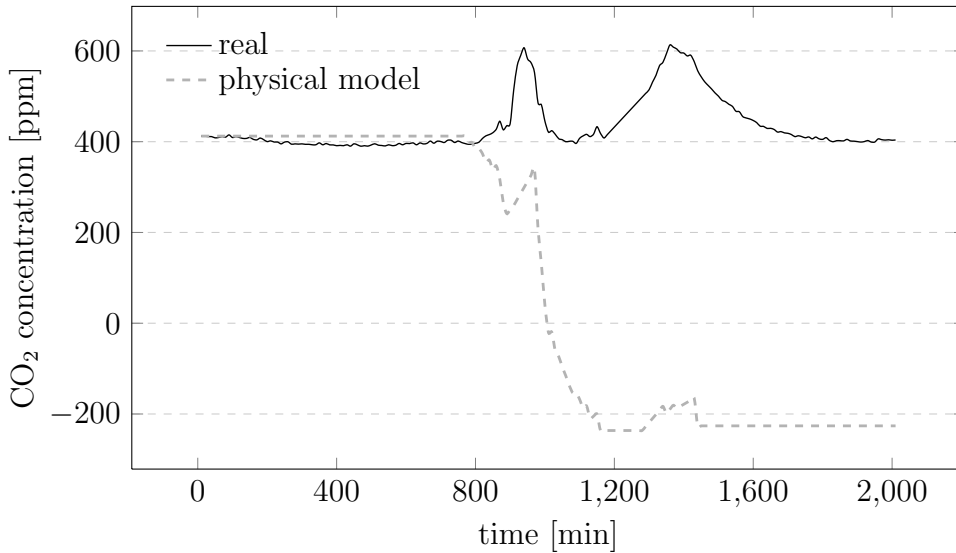


Figure 3.4: Validation of the CO_2 physical model.

model using the well-known Prediction Error Method (PEM) identification technique [40]. The model order was established according to the knowledge of the physical model obtained before. In this sense, a grey-box modeling approach was adopted. Furthermore, adopting simple models permits to obtain

a more flexible design and implementation of the MPC. Hence, we chose an ARX model class, whose general form is

$$A(z^{-1})y(t) = B(z^{-1})u(t) + w(t), \quad (3.11)$$

where $y(t)$ represents the output, $u(t)$ the input, and $w(t)$ noise accounting fitting inaccuracy and prediction errors. First, we assessed the predictive ability of these models when only occupancy is considered. Furthermore, in order to adhere with the physical description of the system, we set the model order to 1-1-1, i.e. one regression coefficient on the output, one on the input and one delay. The model class turned out to be

$$(1 + az^{-1})y(t) = bz^{-1}N_{\text{people}}(t) + w(t) \quad (3.12)$$

Here, the output $y(t)$ represents the CO₂ concentration in the room minus the concentration of CO₂ of fresh air, that is $y(t) = C_{\text{CO}_2}(t) - C_{\text{CO}_2,i} := \Delta_{\text{CO}_2}(t)$. In this way, the dynamics of the system could be captured more properly. As shown in Figure 3.6, we could witness a substantial improvement on the prediction of the concentration of CO₂. Since our final scope is to control the CO₂ level, we needed to consider also the effect of an input, called $u(t)$, which is given by the mass flow incoming into the room with a lower concentration of CO₂. Then the model class that we obtained was

$$(1 + az^{-1})y(t) = b_1z^{-1}u(t) + b_2z^{-1}N_{\text{people}}(t) + w(t) \quad (3.13)$$

where in particular

$$u(t) = \dot{m}_{\text{air}}(C_{\text{CO}_2}(t) - C_{\text{CO}_2,i}) \quad (3.14)$$

Both these models gave a good fitting on the training data set used for the identification process (94.7% e 93.8% respectively for the first and the second formulation); this is shown in Figure 3.5. These model performed well also in the validation phase, where other data were used. The results are shown in Figure 3.6.

In order to complete our analysis, we also tried other type of models, like Output-Error models, which performed worse than ARX. Moreover, we tried to increase the order of the ARX model. However, increasing the order gave worse results in fitting both training and validation data. According with all

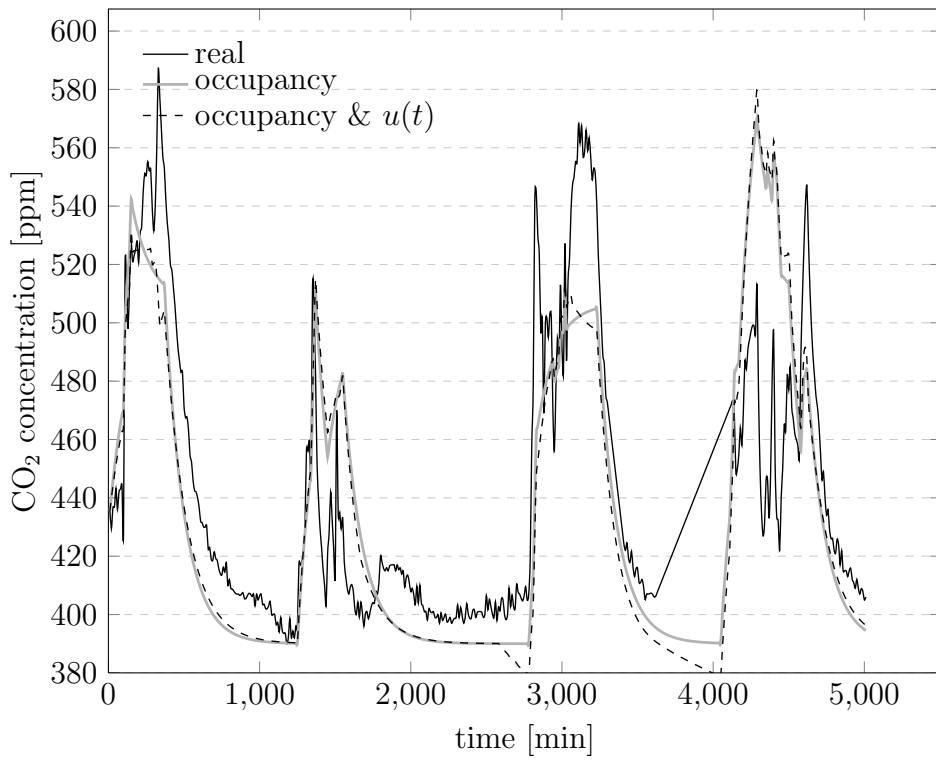


Figure 3.5: Fitting of the CO₂ models with the validation set of data.

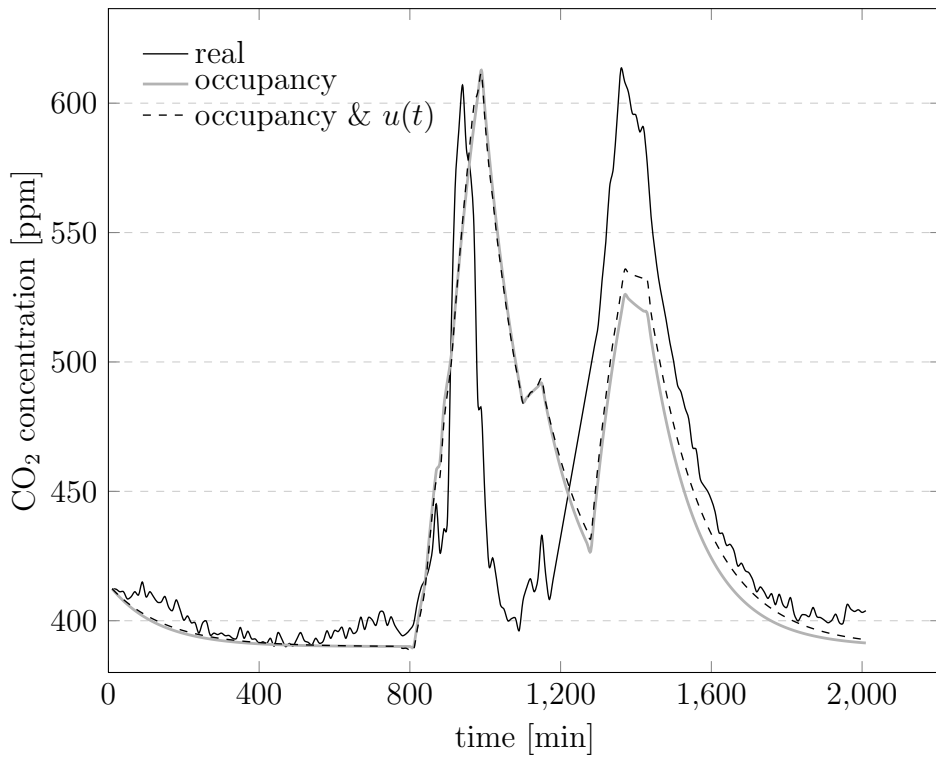


Figure 3.6: Validation of the CO₂ models.

these considerations, the final model for describing the CO₂ concentration is then an ARX111 that accounts for both occupancy and input $u(t)$ of (3.14). A reasonable sample time of the discrete model was 10'. Hence, our adopted model is

$$\Delta_{\text{CO}_2}(t) = +0.9343 \cdot \Delta_{\text{CO}_2}(t-1) - 0.1255 \cdot u(t-1) + 8.9129 \cdot N_{\text{people}}(t-1) + w(t) \quad (3.15)$$

Note that now, when no inputs are given, i.e. no people are in the room and no fresh air is injected, the concentration of CO₂ tends to set to its fresh-air value $C_{\text{CO}_2,i}$. This can be explained by the fact that assuming no leakages in the room is indeed a strong assumption that does not hold in the true system.

Variable	U.M.	Description
α_e	[W/m ² °C]	external heat transfer coefficient
a	[-]	absorption factor for shortwave radiation
A_{rad}	[m ²]	emission area of the radiators
A_{wall}^j	[m ²]	wall area on the j-th surface
A_{win}^j	[m ²]	area of the window on the j-th surface
c	[W]	constant related to equipment and occupants activity
$C_{\text{CO}_2,i}$	[ppmV]	inlet air CO ₂ concentration
C_{CO_2}	[ppmV]	concentration of CO ₂ within the room
c_{pa}	[J/kg° C]	specific heat of the dry air
g_{CO_2}	[m ³ _{CO₂} /pers.]	generation rate of CO ₂ per person
G^j	[-]	G-value (SHGC) of the window on the j-th surface
h_i	[W/m ² °C]	indoor heat transfer coefficient
h_o	[W/m ² °C]	outdoor heat transfer coefficient
h_{rad}	[W/m ² °C]	heat transfer coefficient of the radiators
I^j	[W/m ²]	solar radiation on the j-th surface
$m_{\text{air,zone}}$	[kg]	air mass in the room
\dot{m}_{cool}	[kg/s]	mass flow through the cooling branch
\dot{m}_{vent}	[kg/s]	mass flow through the ventilation branch
N_{people}	[-]	number of occupants in the room
R_{win}^j	[°C/W]	thermal resistance of the window on the j-th surface
T_{ai}	[°C]	air inlet temperature, from the venting outlet
T_{sa}	[°C]	supply air temperature, from the cooling outlet
T_{amb}	[°C]	outdoor temperature
$T_{\text{wall,i}}^j$	[°C]	indoor surface temperature of the wall on the j-th surface
T_{mr}	[°C]	mean radiant temperature of the radiators
V	[m ³]	volume of the air inside the room

Table 3.1: Summary of the parameters involved in the building model.

3.2 Devices to be identified

As shown in the previous section, in order to control our outputs we need a description of some physical features and their connections with our actuation signals. Our actuation on the cooling, venting and heating dumpers (or valves) must be given in terms of percentages. However, we are not aware of the behavior of the physical response of the system. For this reason, we need to test such a behavior.

More precisely, we aim at finding the following features.

- Heating: link the T_{mr} to the valve opening percentage of the radiator.
- Venting: link \dot{m}_{air} , \dot{m}_{vent} and \dot{m}_{cool} to the dampers opening percentage of the venting (inlet and outlet).
- Cooling: find a relationship between T_{sa} and the the valve opening percentage of the cooling.

In the next subsection we present all the tests performed on the testbed.

Test on the average radiant temperature

The first test was made in order to link the mean radiant temperature of the radiators, T_{mr} , and the radiator opening valve percentage. Unfortunately, we could run one test only. This because of a problem with the change of the outdoor weather conditions, which made the main system detect a change from “winter” to “summer”. This interrupted the water flow to the radiator (closing the main valve) and, as shown on Figure 2.5, the water passing through them did not affect the heating of the room. Thanks to Akademiska Hus, we could run one test using water at 46 °C².

We designed a test based on inputs shaped as stairs with steps of size of 20%, each one every 10', from 0% to 100% and then back to 0%. To evaluate the temperature T_{mr} , we put some sensors on the radiators, precisely on the first one and on the last one of the cascade.

We took the mean radiant temperature as the mean of the temperature of these sensors. We also assessed whether a mote positioned in the middle radiator could give the same description with good approximation. An example of sensor placement is in Figure 3.7

²Of course more precise and deep investigations must be done during the winter period



Figure 3.7: Picture of the notes attached to the radiator to run the test to get the mean radiant temperature.

Unfortunately, the results we got were not as expected. A possible reason is given by the dynamics of the system, which might be slower than the one expected. Furthermore, we found delays which need to be investigated accurately. Specifically, we refer to the delay between the actuation and the increasing of the temperature of the radiators, as well as the delays between the actuation of first and the last radiator.

As shown in Figure 3.8 the temperature T_{mr} begins to increase only about 10' after the first actuation command is given. Moreover, we can notice a delay in the temperature growing on each radiator, according to the position of the sensor: the more distant from the hot water inlet the sensor is, the higher the delay is. Notably, the most distant one begins rising after about 25'.

As said before, we found also a delay on the arrival time of the hot water flow between the first and the last radiator. In Figure 3.9 we can see that the sensors placed in the same place on the radiators, like Sensor 1035 and Sensor 1036³, has a delay of about 10'. However, we notice that, when the “steady state” condition is reached, there is a sort of exponential decay similar in both the cases.

We did not need to use any actuation on the radiator, firstly because of

³The notes 1035 and 1036 are placed on the top left corner of the first and last radiator respectively, while notes 1030 and 1037 are placed in the center.

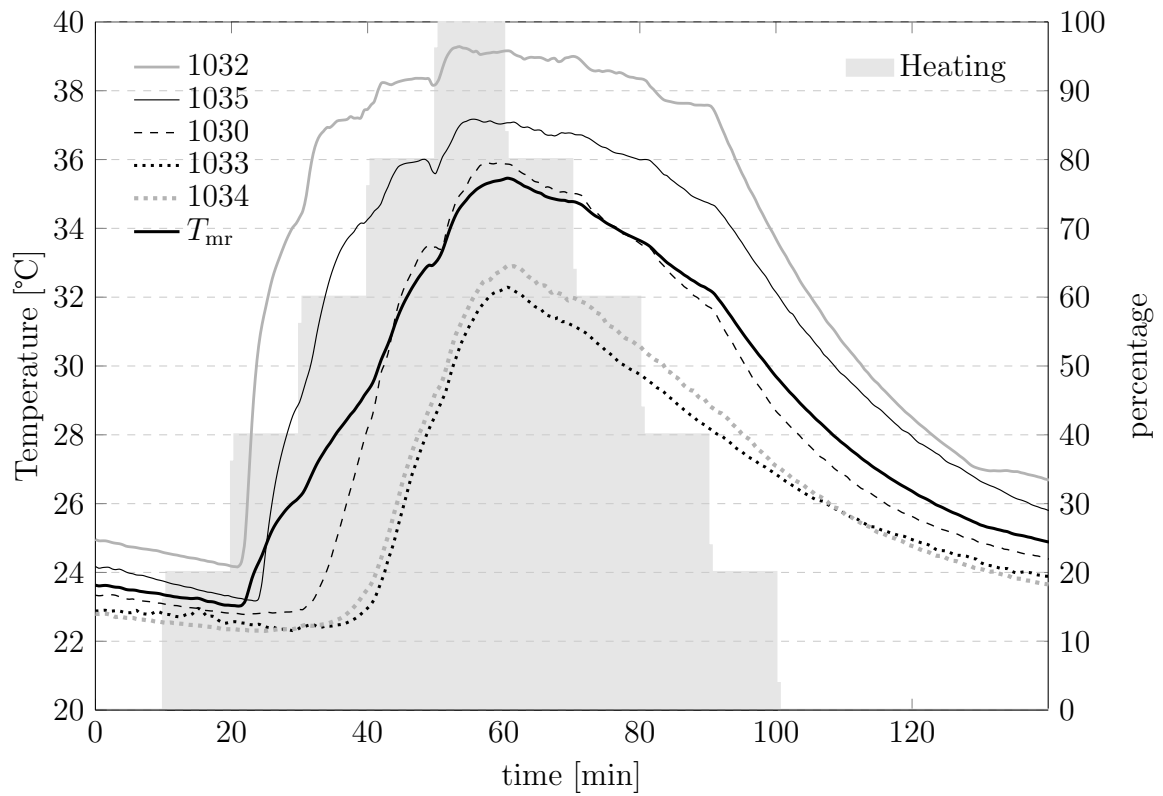


Figure 3.8: Test on the radiators: first radiator temperature response. The notes are placed on the radiator in this order: 1032 on the top right, where there is the hot water inlet, 1035 on the top left, 1030 in the center, 1034 on the bottom left and 1033 on the bottom right, where there is the hot water outlet.

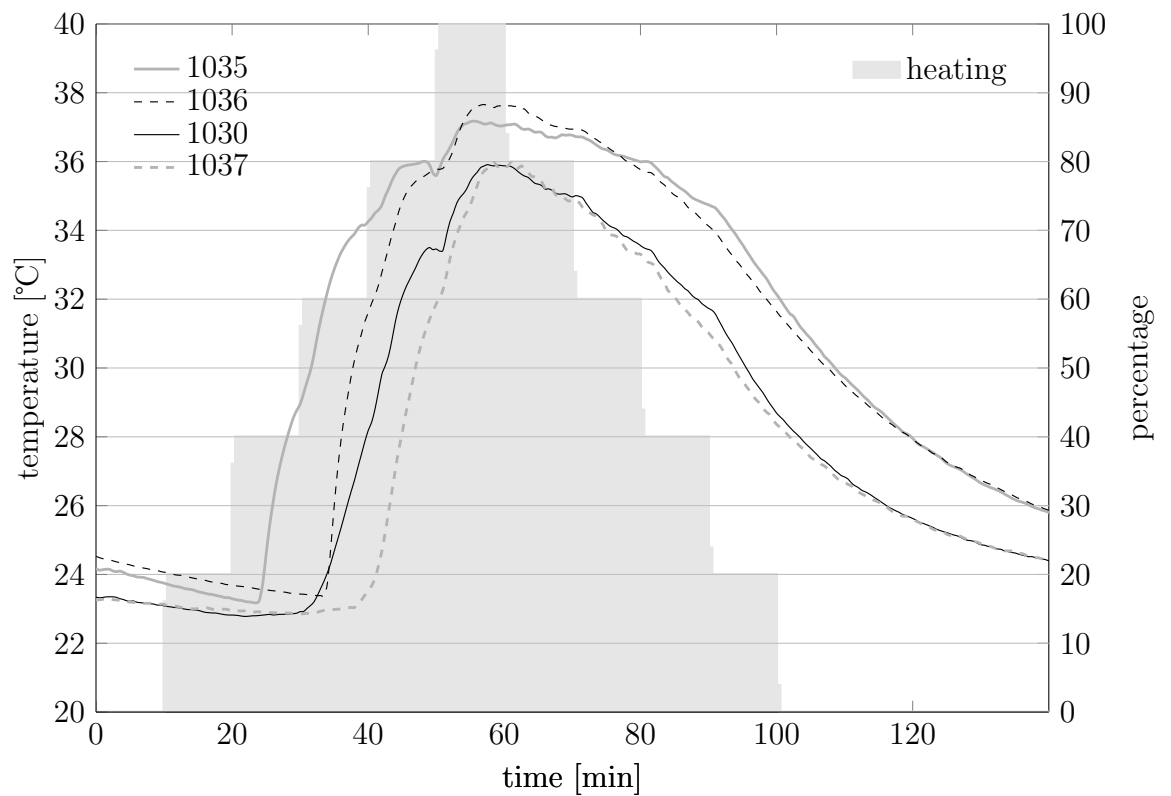


Figure 3.9: Test on the radiators: Comparison between notes in the first radiator (1035, 1030) and in the last (1036, 1037), placed in the same position on the radiator. Motes 1035 and 1036 are placed on the top left corner of the first and last radiator respectively, while Sensor 1030 and Sensor 1037 are placed in the center.

the impossibility of getting hot water during the tests, secondly because we were running our tests during the summer time. What we had to employ was an empirical characterization of the actuation command, considering the temperature of the hot water. However, for our final goal this was insufficient, thus the first step must be repeated for obtaining an improvement.

Test on the air inlet mass flow

In this subsection we seek for a relation between the opening valve percentage of the dumper of the ventilation system ($A_v(t)$) and the air mass flow actually carried into the room ($\dot{m}_{air}(t)$).

Our understanding of the ventilation system control design leads us to deduce that this relation has to be approximately linear. A linear-quadratic relation with a small coefficient on the quadratic term is also considered.

As explained in Section 2.2 the ventilation duct that comes in the testbed is split in two equal branches with the same characteristics, and accordingly with the same air mass flow⁴. Both the branches are in turn split in two parts: one part for the cooling system and one for the ventilation. Thus, we can write

$$\dot{m}_{air}(t) = \dot{m}_{vent}(t) + \dot{m}_{cool}(t) \quad (3.16)$$

where $\dot{m}_{vent}(t)$ is the part of air mass flow for the ventilation system and $\dot{m}_{cool}(t)$ is the one for the cooling system.

We decided to measure the air mass flow (both in the cooling duct and the venting duct) at four different percentages of valve opening (30%, 50%, 70% and 100%). We attempted to build a map assuming that there is no dynamic features behind, i.e. the opening of the valve reaches immediately the corresponding air mass flow⁵.

These measurements were made, thanks to the support of a technician, using an anemometer. We measured the average air velocity ($v_{air} \left[\frac{m}{s} \right]$), by

⁴It seems reasonable, due to the symmetric geometry of the system and the operating conditions of the ventilation system, to assume that the branches are specular. The measurements have then been carried out only on one branch. According to the previous assumptions, the total air flow is twice the air flows in the measured branch

⁵This assumption has been done because the time constant to reach the steady state values are considerably small compared to the other time constants of the system

means of which we estimated the volumetric air flow ($Q_{\text{air}} \left[\frac{\text{l}}{\text{s}} \right]$)

$$Q_{\text{air}} = v_{\text{air}} \cdot A_{\text{pipe}} \left[\frac{\text{l}}{\text{s}} \right] \quad (3.17)$$

In the above formula, A_{pipe} represents the area of the section of the pipe⁶. The diameters of the cooling pipe and of the venting pipe are 0.16m and 0.20m respectively. The air mass flow is then the given by

$$\dot{m} = 2 \cdot Q_{\text{air}} \cdot \rho \left[\frac{\text{kg}}{\text{s}} \right] \quad (3.18)$$

where $\rho \simeq 1.225 \frac{\text{kg}}{\text{m}^3}$ is the air density, and the scalar 2 is due to the fact that we have two equal branches. The results we found are summarized in the Table (3.2)

Valve	Cooling branch			Venting branch			Total
A_v	v_{cool}	Q_{cool}	\dot{m}_{cool}	v_{vent}	Q_{vent}	\dot{m}_{vent}	\dot{m}_{air}
0%	0	0	0	0	0	0	0
30%	1.25	0.0251	0.0605	1.75	0.0550	0.1324	0.1929
50%	1.65	0.0332	0.0799	2.46	0.0773	0.1861	0.2660
70%	1.99	0.0400	0.0963	2.76	0.0867	0.2088	0.3051
100%	2.39	0.0481	0.1157	3.63	0.1140	0.2746	0.3903
M.U.	$\left[\frac{\text{m}}{\text{s}} \right]$	$\left[\frac{\text{l}}{\text{s}} \right]$	$\left[\frac{\text{kg}}{\text{s}} \right]$	$\left[\frac{\text{m}}{\text{s}} \right]$	$\left[\frac{\text{l}}{\text{s}} \right]$	$\left[\frac{\text{kg}}{\text{s}} \right]$	$\left[\frac{\text{kg}}{\text{s}} \right]$

Table 3.2: Measurements for the air velocity and the corresponding volumetric air flows and mass flow of the branches, where A_v is the venting valve opening percentage.

With the available data, and with the knowledge that the plant was built to give a possibly linear response, we decided to fit this value using a linear relation. However this solution was not really precise and gave a large fitting error. For this reason we decided to use a quadratic function to interpolate our measurements. In order to fit the data we used the embedded Matlab tool *cftool*. The result obtained are shown in Figure (3.10); the parabolic functions we found are of the form

$$\dot{m}_{\text{cool,vent,air}} = a_{c,v,\text{air}} \cdot A_v^2 + b_{c,v,\text{air}} \cdot A_v + c_{c,v,\text{air}} \quad (3.19)$$

⁶Because of the geometry of the pipes, that are straight, we can assume that the average air velocity is exactly the one we measured

where

$$\begin{aligned} a_c &= -9.789 \cdot 10^{-6} & b_c &= 0.002118 & c_c &= 0 \\ a_v &= -1.885 \cdot 10^{-5} & b_v &= 0.004564 & c_v &= 0 \\ a_{\text{air}} &= -2.8639 \cdot 10^{-5} & b_{\text{air}} &= 0.006682 & c_{\text{air}} &= 0 \end{aligned} \quad (3.20)$$

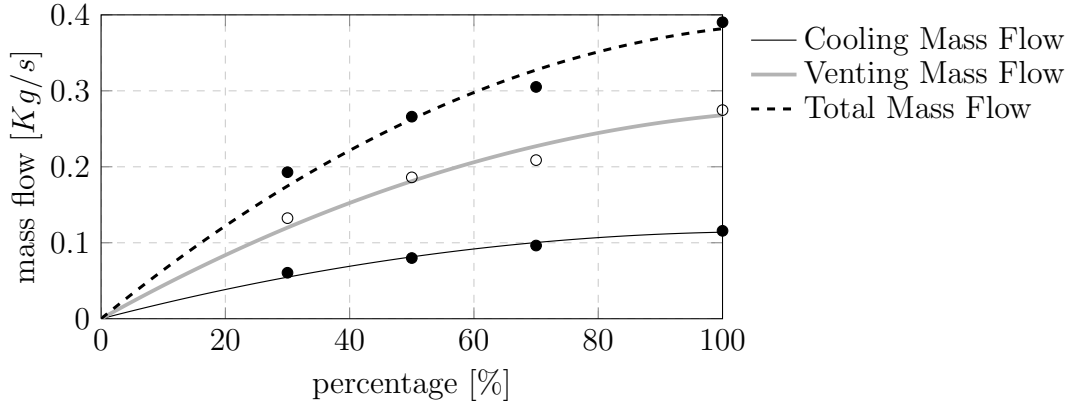


Figure 3.10: Relation between mass flow and opening valve percentage

Clearly, in order to obtain the opening percentage needed for having a given mass flow amount, we can simply use the inverse formula⁷, obtaining

$$A_v = -\frac{b - \sqrt{b_{c,v,\text{air}}^2 - 4 \cdot a_{c,v,\text{air}} \cdot c_{c,v,\text{air}} + 4 \cdot a_{c,v,\text{air}} \cdot \dot{m}_{\text{cool,vent,air}}}}{2 \cdot a_{c,v,\text{air}}} \quad (3.21)$$

Temperature of the air coming out from the AC

As explained in Section 2.2, the air provided by the ventilation system, at a temperature that is uncontrollable, and the air within the room, kept by convective motions, are cooled by a chiller coil placed just before the AC outlet.

We assessed that the temperature of the air conditioning ($T_{sa}(t)$) could be modelled by using a linear regression that could include a part of its past values and other system variables that may affect its behavior, i.e. the chilled water circuit valve opening percentage ($A_c(t)$), the venting inlet valve opening percentage ($A_v(t)$) and the temperature of the air that the ventilation duct provided to the cooling system ($T_{ai}(t)$).

More precisely, given the Nonlinear-ARX (NARX) model

$$T_{sa}(t+1) = \alpha T_{sa}(t) + \beta T_{sa}(t-1) + \gamma A_c(t) + \delta A_c(t) A_v(t) + \epsilon T_{ai}(t) \quad (3.22)$$

⁷We need to be careful to choose the correct root of the quadratic equation

the identification problem can be solved by solving the optimization problem

$$\min_{\alpha\beta\gamma\delta\epsilon} \|Ax - b\|_2 \quad (3.23)$$

where the matrix giving the one step predictors is

$$Ax = \begin{bmatrix} T_{sa}(1) & T_{sa}(0) & A_c(1) & A_c(1)A_v(1) & T_{ai}(1) \\ T_{sa}(2) & T_{sa}(1) & A_c(2) & A_c(2)A_v(2) & T_{ai}(2) \\ \vdots & \vdots & \vdots & \vdots & \vdots \\ T_{sa}(k) & T_{sa}(k-1) & A_c(k) & A_c(k)A_v(k) & T_{ai}(k) \\ \vdots & \vdots & \vdots & \vdots & \vdots \end{bmatrix} \begin{bmatrix} \alpha \\ \beta \\ \gamma \\ \delta \\ \epsilon \end{bmatrix}, \quad (3.24)$$

the matrix of measurements is

$$b = \begin{bmatrix} T_{sa}(2) \\ T_{sa}(3) \\ \vdots \\ T_{sa}(k+1) \\ \vdots \end{bmatrix} \quad (3.25)$$

and $\|\cdot\|_2$ is the 2-norm.

The data used for the identification are from time 15:00 of May, 8th up to time 12:00 of May, 10th. The sampling time of the values is 60s; in order to be sure that the samples are synchronized, a resampling was been done. The commands given to the actuators are the standard ones, decided by the default controller (see 2.2). The set of data was divided in two parts; the first was used as training set to identify the model, while the second was employed as test set, in order to validate the model previously found. The validation was done by setting the initial condition to the ones of the real data and evaluating the response of the system, using the true input signals, in term of fitting the real response⁸.

The fitting score is calculated by means of the following expression

$$Fit = \left(1 - \frac{\|T_{sa} - \hat{T}_{sa}\|_2}{\|T_{sa}\|_2} \right) \times 100. \quad (3.26)$$

⁸Actually, to be sure of the results, we test it also in the whole period and also in other data sets. However, here we prefer not to add more results to keep the presentation brief.

Furthermore, in order to obtain more accurate scores we also evaluated the index

$$Fit_m = \left(1 - \frac{\| (T_{sa} - \bar{T}_{sa}) - (\hat{T}_{sa} - \bar{\hat{T}}_{sa}) \|_2}{\| T_{sa} - \bar{T}_{sa} \|_2} \right) \times 100 \quad (3.27)$$

where T_{sa} is the vector with the real response of the system, whose mean is \bar{T}_{sa} , and \hat{T}_{sa} is the vector with the response of the identified system, whose mean is $\bar{\hat{T}}_{sa}$.

The parameters that were found are

$$\alpha = 1.4250 \quad \beta = -0.4564 \quad \gamma = -1.5590 \cdot 10^{-3} \quad \delta = 8.8073 \cdot 10^{-6} \quad \epsilon = 0.0303 \quad (3.28)$$

With these parameters the fitting score were

$$Fit = 98\% \quad Fit_m = 73\% \quad (3.29)$$

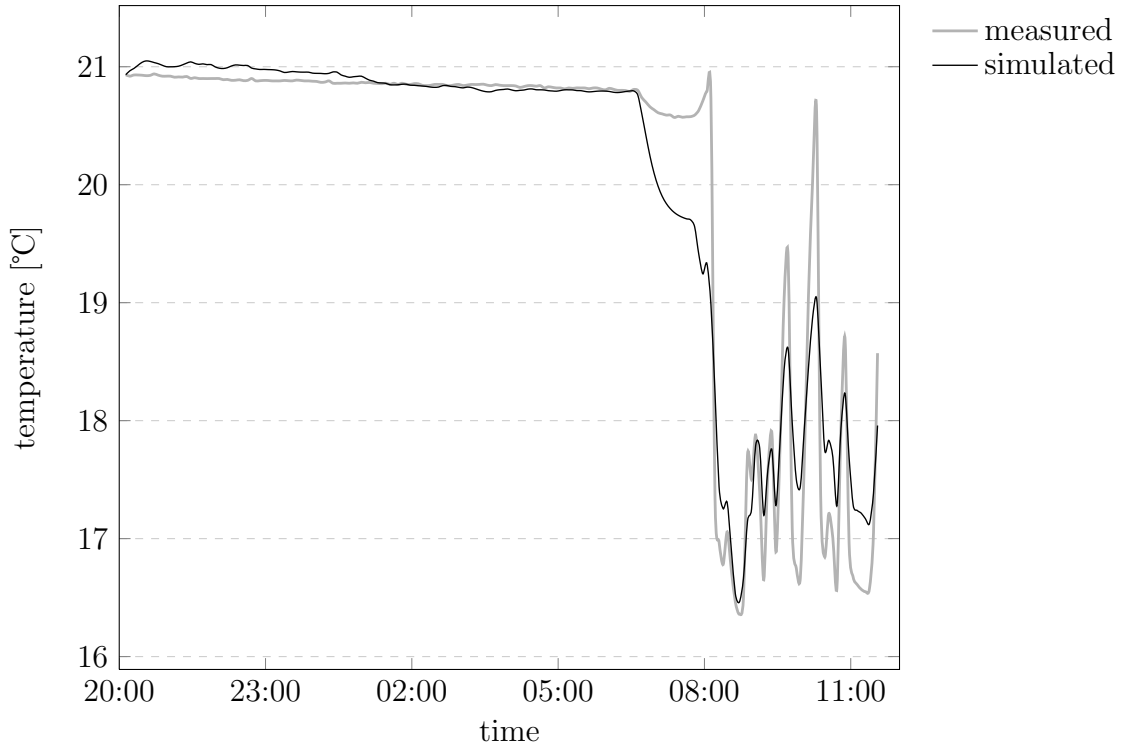


Figure 3.11: Fitting between real supply air temperature of the air conditioning outlet and the simulated one.

It is reasonable to consider this model as a good approximation of the real

behavior of the temperature of the air coming from the air conditioning system, and use it in our control system.

4

Control strategies

This section describes the main control strategies considered in the thesis.

4.1 The current practice Proportional Integrative (PI) controller

Compared to the majority of the buildings in Stockholm, the Q building (where the testbed is placed) is very energy efficient, and presents many advanced technological solutions. Nonetheless, as already described in Section 2.2, the system operator (Akademiska Hus) chose to control the HVAC system by means of simple Proportional Integrative (PI) controllers. More precisely, there are two different PIs, designed to act on different components: one for managing the temperature and one for managing the CO₂ levels:

temperature controller: unfortunately complete documentation on the structure and parameters of this controller is missing: from the information received from Akademiska Hus the temperature controller in winter exploit radiators and in summer the air cooling system. This controller works only when the temperature of the room does not lay in a comfort

band that represents the desired temperature range. From practical perspectives the control strategy is not endowed with temperature reference signals, but rather reference band. It is indeed a dead zone controller: if the temperature is inside the comfort band then no control actions are taken. More precisely, during summer the band is defined by the interval $[21 - 23]^{\circ}\text{C}$. If the measured temperature does not belong to this interval then the PI controller starts actuating to bring the temperature back to this dead zone. The control commands are computed with a frequency of one command per second. We notice that this control strategy does not take into account neither energy efficiency nor actuators wear indexes;

CO₂ levels controller: this controller actuates only the ventilation system. The control strategy is similar to the previous one, with the CO₂ ppm levels dead zone that ranges from 0 to 850.

Figure 4.1 shows some measured behaviors of the two previously mentioned controllers. We can notice that sometimes the behavior of the actuation signals do not follow the rules suggested by Akademiska Hus. Moreover the previously described comfort bounds are not always respected: we indeed noticed that sometimes the temperature violation is as big as half Celsius degree.

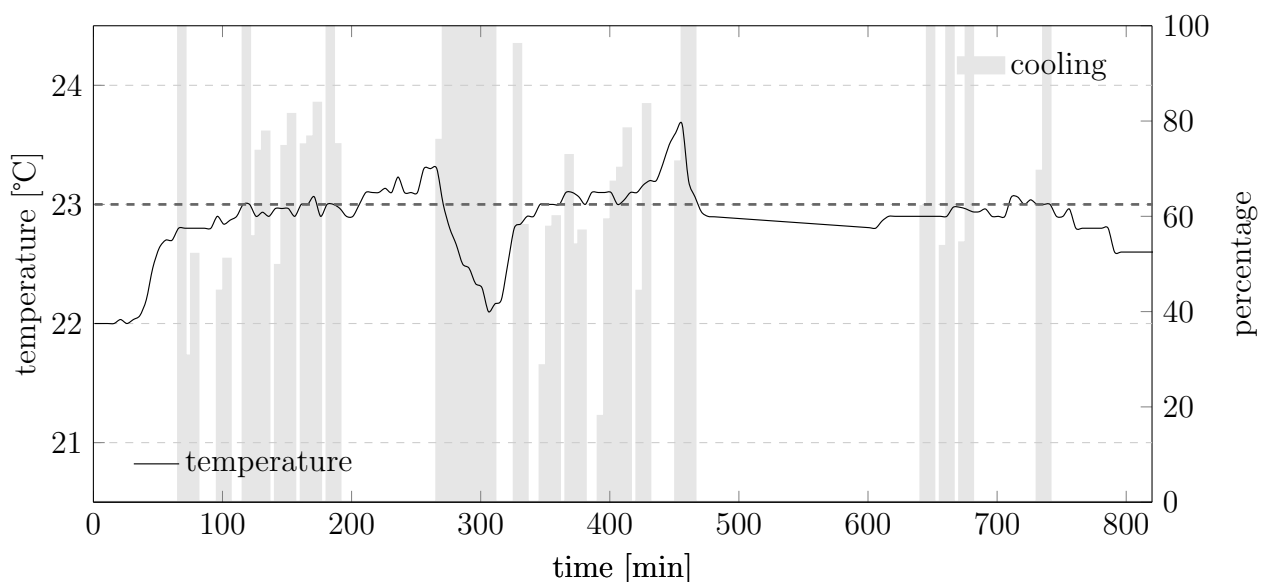


Figure 4.1: Example of the actuation signals induced by the Akademiska Hus PI controller: cooling action.

4.2 The considered Model Predictive Control (MPC) strategy

The current section describes the MPC strategy that has been implemented in the testbed. It starts by defining the strategy in a formal and generic way, and then considers the tailored algorithm used for our experimental evaluation purposes.

Preliminaries on mathematical optimization problems

A mathematical optimization problem can generally be written as find the values of some variables that maximize or minimize a given cost or reward, subject to some limitations (also called constraints) on these variables [41]. Formally,

$$\begin{aligned} z^* = \arg \inf_z \quad & f(z) \\ \text{subject to} \quad & z \in S \subset Z \end{aligned} \quad (4.1)$$

where z represents the decision variables, Z represents the set of the meaningful decision variables, $S \subseteq Z$ is the set of plausible (formally, feasible or admissible) decision variables, and z^* is that (possibly non-unique or even not-existing) value of the decision variable that minimizes the costs. Solving (4.1) leads also to compute

$$J^* := \inf_{z \in S} f(z), \quad (4.2)$$

i.e., the optimal cost (formally, the biggest lower bound of $f(z)$ over the set S). If $J^* = -\infty$ we say that the problem is unbounded below. If the set S is empty then the problem is said to be infeasible and we set $J^* = +\infty$ by convention. If $S = Z$ then the problem is said to be unconstrained.

If z^* in (4.1) is not unique, one is in general interested in finding one of the instances of these optimal variables. In this case the following equality holds:

$$J^* = \min_{z \in S} f(z). \quad (4.3)$$

Moreover in this case z^* is said to be a (global) optimizer.

Continuous optimization problems: in this particular case the domain Z is an Euclidean space. Assume the dimensionality of this domain to be s , so

that $Z \subseteq \mathbb{R}^s$. It is then usual to rewrite problem (4.1) as

$$\begin{aligned} & \inf_z && f(z) \\ & \text{subject to} && g_i(z) \leq 0 \quad \text{for } i = 1, \dots, m \\ & && h_i(z) = 0 \quad \text{for } i = 1, \dots, p \\ & && z \in Z \end{aligned} \tag{4.4}$$

where $f, g_1, \dots, g_m, h_1, \dots, h_p$ are functions defined over \mathbb{R}^s . In this case Z represents the intersection of the domains of the cost f and of the constraint functions g_i, h_i . If these constraint functions are not present, i.e., if $m = p = 0$, and the domain of f is the whole \mathbb{R}^s then the problem is unconstrained.

The inequalities $g_i(z) \leq 0$ are called *inequality constraints* and the equations $h_i(z) = 0$ are called *equality constraints*. $\bar{z} \in \mathbb{R}^s$ is said to be *feasible* for (4.4) if it belongs to Z and it satisfies all the inequality and equality constraints, i.e., if $g_i(\bar{z}) \leq 0, i = 1, \dots, m, h_i(\bar{z}) = 0, i = 1, \dots, p$.

The standard optimization problem (4.4) is said to be convex if the cost function f is convex on Z and S is a convex set.

Definition 1 (Convex set). A set $S \in \mathbb{R}^s$ is convex if

$$\lambda z_1 + (1 - \lambda)z_2 \in S \quad \text{for all } z_1, z_2 \in S, \lambda \in [0, 1] \tag{4.5}$$

Definition 2 (Convex function). A function $f : S \rightarrow \mathbb{R}$ is convex if S is convex and

$$\begin{aligned} f(\lambda z_1 + (1 - \lambda)z_2) & \leq \lambda f(z_1) + (1 - \lambda)f(z_2) \\ & \text{for all } z_1, z_2 \in S, \lambda \in [0, 1] \end{aligned} \tag{4.6}$$

Very importantly, convex optimization problems are s.t. local optimizers are always also global optimizers. This is not guaranteed for non-convex optimization problems, for which finding minima do not imply to find the best possible solution.

In this thesis we rely on two famous numerical optimization software tools: *CPLEX* and *CVX*. *CPLEX* [42], developed by IBM, is a high-performance mathematical solver that handle linear programming, mixed integer programming, and quadratic programming problems. *CVX* [43] is instead a Matlab-based

tool designed for disciplined Convex Programming and developed by CVX Research Inc.

Preliminaries on Model Predictive Control (MPC)

MPC [44, 41] is a simple and intuitive approach to perform constrained control. During each sampling interval, a finite horizon optimal control problem is formulated and solved over a finite future window. The result is a trajectory of inputs and states into the future that satisfy the dynamics and constraints of the system while optimizing some given criteria.

In terms of building control, this means that at the current point in time, a heating / cooling / venting plan is formulated for the next next future (from horizons that can span from several hours to days). This plan accounts for the predicted weather conditions, disturbances (e.g., internal gains given by occupants), time-dependencies of the control costs (e.g., dynamic electricity prices), and constraints (e.g., thermal comfort ranges). Once this plan is computed by solving an opportune constrained optimization problem, only the first step of this plan is applied. Then the window is shifted backwards by one step, a further time step is added at the end of the window, and the process is repeated at the next sample.

The receding horizon is actually what introduces feedback into the system: indeed, the optimal control problem solved at time t is a function of the state at time t and of the disturbances acting on the system up to time t . Figure 4.2 summarizes the previous discussion. The modeling and design efforts consist of specifying some dynamics, constraints of the control problem and a cost function that encapsulates the preferences of the user towards some particular behavior of the control signals (e.g., keep them as small as possible because they are associated with energy consumptions, or keep them as constant as possible since changes are associated to undesired wear). In each sampling interval, these components are combined and converted into an opportune optimization problem. A generic framework is given by the following

$$\begin{aligned}
 \min_{u_0, \dots, u_{N-1}} \quad & p(x_N) + \sum_{i=0}^{N-1} q(x_i, u_i, r_i) & (1) \text{ Cost function} \\
 \text{subject to} \quad & x_0 = x & (2) \text{ Current state} \\
 & x_{i+1} = f(x_i, u_i) & (3) \text{ Dynamics} \\
 & (x_i, u_i) \in \mathbb{X}_i \times \mathbb{U}_i & (4) \text{ Constraints}
 \end{aligned} \tag{4.7}$$

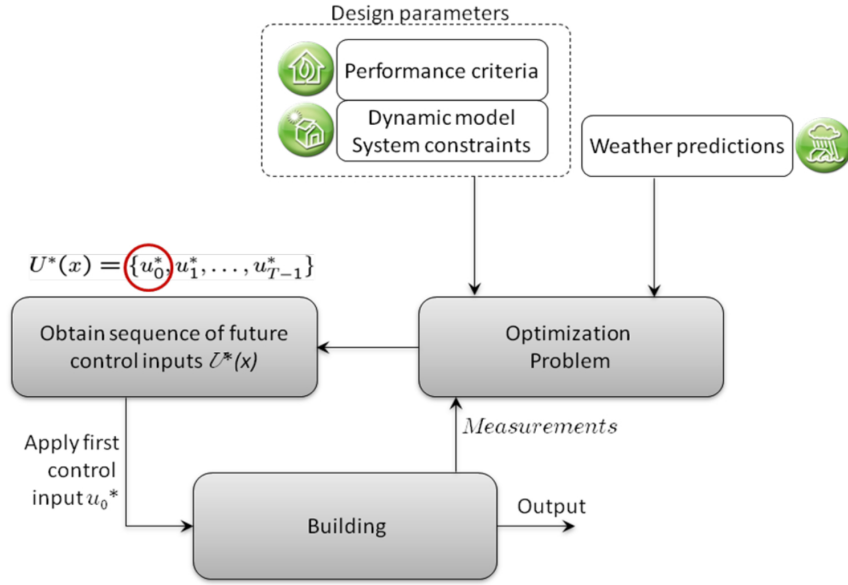


Figure 4.2: Basic description of the main functioning of a Model Predictive Control (MPC) scheme [44].

Cost functions

The cost functions (abbreviated often with “cost”) generally serve two purposes: induce *stability* in the plant and describe the *performance indexes*. Stability is achieved by choosing costs that are Lyapunov functions for the closed loop system. In practice, this requirement is generally relaxed for stable systems with slow dynamics, such as buildings, and this increases the freedom to select the cost strictly on a performance index basis. Costs are generally, but not always, used to specify a preference for one closed-loop behavior over another. E.g., one may prefer to achieve minimum energy instead of maximum comfort. It is nonetheless common to describe costs as convex combinations of these performance indexes.

Reflecting the fact that this induces simpler optimization problems, the majority of the most common cost functions are convex. Examples are:

$$\begin{aligned}
 \text{Quadratic costs,} & \quad q(x_i, u_i) = x_i' Q x_i + u_i' R u_i \\
 \text{Integral costs,} & \quad q(x_i, u_i) = \|u_i\|_1 \\
 \text{Probabilistic costs,} & \quad q(x_i, u_i) = \mathbb{E}[g(x_i, u_i)].
 \end{aligned} \tag{4.8}$$

Quadratic regulators (or trackers) are s.t. the relative weighting between the states and the inputs provides a trade-off between regulation quality and energy of the inputs. If the system is unconstrained, or the constraints are not

active, then the problem reduces to a classic Linear Quadratic Regulator (LQR). In the context of building control scenarios, such a cost would generally only be used at the lowest level to replace, for example, existing PIs or rule-based controllers.

Integral costs, instead, weight the integral of the energy of the inputs. This is a common choice whenever the performance index is the minimization of the used energy.

Probabilistic costs are eventually tailored for system subject to random disturbances. In this way users may choose to take into account the stochastic nature of certain phenomena, and to minimize some expected value of some event (or transformation of events), such as room comfort bounds violations.

Dynamics

The dynamics of the to-be-controlled system are represented by two distinct parts: the initial conditions and the time evolution.

General MPC strategies require to initialize the model of the system at each time step. This is performed usually by forcing the state of this system to be equal to the measured / estimated current state. In this way all the future control predictions begin from a system that is initialized every time in a different way. We also notice that this strategy is not the unique one: certain robust MPC strategies for example assume the current state to be not known exactly, but only to belong to a bounded set.

Assuming the initial conditions to be set, to predict the future states numerical optimizers need a model of the evolution of the system. Modeling the dynamics of the system plays a critical role in MPC frameworks: indeed, if the model of the temporal evolution of the plant is grossly mistaken then the numerical optimizers will return control plans that may eventually lead to very poor control performance. The most common models considered in MPC

schemes are:

$$\begin{array}{ll}
 \text{Linear} & x_{i+1} = Ax_i + Bu_i \\
 \text{Input-Affine} & x_{i+1} = f(x_i) + g(x_i)u_i \\
 \text{Hybrid} & x_{i+1} = \begin{cases} A_1x_i + B_1u_i & \text{if } x_i \in P_1 \\ \vdots \\ A_nx_i + B_nu_i & \text{if } x_i \in P_n \end{cases} \\
 \text{Non-Linear} & x_{i+1} = f(x_i, u_i)
 \end{array} \tag{4.9}$$

Linear models are of course the most common models. Importantly, they are the only one that lead to a convex and easily solvable optimization problem.

Input-affine models can instead cover a large number of very complex systems, at the price of being in general very difficult to handle. We nonetheless notice that there are recent theories that in some circumstances provide very simple and stabilizing recipes. As explained later in Section 3.1, our building model belongs to this class, since it contains a bilinear term between the states and the inputs. We then notice that such a model admit some mathematical tricks that allow efficient management of their dynamics.

Hybrid models, in this case piecewise affine (PWA) models, contain a mixture of discrete and continuous components, such as switches or valves in combination with continuous systems. This class of models is extremely general and can be used to approximate any smooth system to an arbitrary degree of accuracy. Optimization problems defined over this class of systems involve treating mixed-integer values. The corresponding optimization problems are generally hard to be solved, although many well-tested methods are available for some special cases.

Non-linear models are the most general models. Due to their generality they are significantly more difficult to handle and thus (a part some specific examples) not considered for MPC purposes.

Constraints

The strength of the MPC approach is in the ability of specifying constraints that are handled directly by the optimization routines. The most commonly

used types of constraints are:

$$\begin{aligned}
 &\text{Linear constraints,} && Ax_i \leq b \\
 &\text{Convex quadratic constraints,} && (x_i - \bar{x})^\top P(x_i - \bar{x}) \leq 1 \\
 &\text{Second order cone constraints,} && \|Ax_i + b\|_2 \leq c \\
 &\text{Chance constraints,} && P(Ax_i \leq b) \leq \alpha, \mathbb{E}[Ax_i] \leq b.
 \end{aligned} \tag{4.10}$$

The most widely used constraints are the linear (or polyhedral) ones. They are generally used to specify upper/lower bounds on the various system variables. They can also be used to approximate non-linear convex constraints to an arbitrary degree of accuracy. Linear constraints also result in the simplest optimization problems. Convex quadratic bounds correspond to ellipses, while chance constraints limit the probability that a bound will be violated. Second order cone constraints, instead, bound the 2-norm of a linear function of the state or input. They are typically used in several forms of stochastic MPCs.

The MPC implemented in the testbed

The previous section provided a general description of MPC strategies. We now describe our implementation choices.

We follow a peculiar MPC approach, named Certainty Equivalence MPC. More precisely:

- the cost function weights the integral of all the control actions;
- the dynamics of the system is assumed linear;
- the constraints represent the upper and lower bounds on the inputted energy, the possible actuator ranges (e.g., the valve opening percentages, that must be restricted in the range 0% to 100%), or the various comfort requirements for the room temperature, the indoor air quality. All these constraints are assumed linear;
- the forecasts are assumed as certain. I.e., the forecast are deterministic quantities.

The MPC accounts for two specific problems: to bound the CO₂ concentration and the indoor temperature levels inside certain comfort ranges. As a consequence we design two separated MPC problems that work in cascade:

the first is dedicated to the management of the CO₂ levels. The second to the temperature. The first targets to return the minimal level of fresh air flow that must enter in the room to maintain a certain comfort range. The second instead computes the actuation commands to let the temperature be in its comfort range.

The main performance index considered while designing the cost functions is the amount of energy spent to maintain the internal comfort levels. The optimization routines thus aim to find the control references that satisfy the air quality levels while spending the least amount of energy. We also notice that we consider two separated MPCs to obtain linear models, exploiting the fact that the dynamics of the CO₂ levels is decoupled from the one of the temperature.

The designed MPC cycles the following steps:

1. build a model of the physical variables of interest (if it changes at each sample time);
2. take the local measurements;
3. build weather / occupancy / solar radiation predictions;
4. build the MPC formulation and construct the constraints;
5. solve the linear problem deriving from the previous step;
6. apply the computed control actions (only the first sample, in accordance with the MPC paradigm);
7. wait the next sample time and repeat the procedure.

The models (3.3) and (3.15) described in Section 3.1 contain nonlinearities that can lead to intractable problems. To address this issue we derive linear equivalent formulations of the CO₂ concentration model (in Section 3.1) and of the room thermal model (in Section 3.1).

The CO₂ MPC

To linearize the CO₂ concentration dynamics, as already considered in (3.15) and also in the identification that carried to that expression, we replace the nonlinear term $\dot{m}_{\text{air}} \cdot (C_{\text{CO}_2} - C_{\text{CO}_2,i})$ with u_{CO_2} , where $C_{\text{CO}_2,i}$ is the concentration of the air that is flowing inside. We can consider it like a constant (with the

value of the CO₂ in the outside environment, around 390 ppm). Since $C_{CO_2,i}$ is the minimum level that the indoor air may have, $C_{CO_2} - C_{CO_2,i}$ is a nonnegative variable. Hence, the CO₂ concentration dynamics can be described by the discrete LTI system

$$\begin{aligned} x_{CO_2}(k+1) &= ax_{CO_2}(k) + bu_{CO_2}(k) + ew_{CO_2}(k) \\ y_{CO_2}(k) &= x_{CO_2}(k), \end{aligned} \quad (4.11)$$

where

$$x_{CO_2}(k) = C_{CO_2}(k) - C_{CO_2,i}$$

is the state, and

$$w_{CO_2}(k) = N_{\text{people}}(k)$$

is the disturbance at time step k . In this case a, b, e are appropriate scalars which values are the one identified in (3.15).

The MPC problem can then be formulated as:

Problem 3 (Formulation of the MPC for the CO₂ concentration).

$$\begin{aligned} \min_{u_{CO_2}(t), \dots, u_{CO_2}(t+N-1)} \quad & \sum_{k=t}^{t+N-1} u_{CO_2}(k) \\ \text{subject to} \quad & \underline{u}(k) \leq u_{CO_2}(k) \leq \bar{u}(k) \quad k = t, \dots, t+N-1 \\ & y(k) \leq \bar{y} \quad k = t, \dots, t+N-1 \end{aligned}$$

where

$$\begin{aligned} \underline{u}(k) &= \dot{m}_{\text{air}}^{\min} \cdot x_{CO_2}(k) \\ \bar{u}(k) &= \dot{m}_{\text{air}}^{\max} \cdot x_{CO_2}(k) \\ \bar{y} &= C_{CO_2}^{\max} - C_{CO_2,i} \end{aligned}$$

with t is the current point in time, N is the prediction horizon and $C_{CO_2}^{\max}$ is equal to the desired upper bound of the CO₂ concentration.

In Problem 3 the constraints can be written as

$$\begin{aligned} g_{u,CO_2}u(k) + g_{x,CO_2}x(k) &\leq g_{CO_2} \\ y_{CO_2}(k) &\leq \bar{y}. \end{aligned} \quad (4.12)$$

Considering the dynamics of the CO₂ model it follows that

$$x_{CO_2}(k) = y_{CO_2}(k) = a^k x_{CO_2 0} + \sum_{i=0}^{k-1} a^{k-i-1} b u_{CO_2}(i) + \sum_{i=0}^{k-1} a^{k-i-1} e w_{CO_2}(i).$$

Thanks to the previous model we can derive the matrices to be given to the subsequent CO₂-MPC problem. For the sake of brevity and exposition clarity we omit to write all the passages in detail. Eventually, the control variable \dot{m}_{air} can be computed by means of the inverse formula

$$\dot{m}_{\text{air}}(k) = \frac{u_{CO_2}(k)}{C_{CO_2}(k) - C_{CO_2,i}}.$$

The Temperature MPC

Considering the model presented in Section 3.1 we can express the heat due to the ventilation and the cooling as

$$\begin{aligned} Q_{\text{air}} &= Q_{\text{vent}} + Q_{\text{cool}} = \dot{m}_{\text{vent}} c_{\text{pa}} \Delta T_{\text{vent}} + \dot{m}_{\text{cool}} c_{\text{pa}} \Delta T_{\text{cool}} = \dot{m}_{\text{air}} c_{\text{pa}} \Delta T_{\text{air}} \\ &= \dot{m}_{\text{air}} c_{\text{pa}} (T_{\text{air}} - T_{\text{room}}) = \dot{m}_{\text{air}} c_{\text{pa}} (\Delta T_h - \Delta T_c) = c_{\text{pa}} (u_h - u_c), \end{aligned} \quad (4.13)$$

where T_{air} is considered to be a mix of the temperatures of the air from the venting outlet, of T_{ai} , and of the air coming from the cooling outlet, T_{sa} .

It is important to comment the meaning of the nonnegative variables ΔT_h , ΔT_c , u_h and u_c . If we use only the ventilation system then T_{sa} is equal to the temperature of the venting duct, and thus $T_{\text{sa}} = T_{\text{ai}}$. In this case thus

$$Q_{\text{air}} = \dot{m}_{\text{air}} c_{\text{pa}} \Delta T_{\text{vent}} = \dot{m}_{\text{air}} c_{\text{pa}} (T_{\text{ai}} - T_{\text{room}}), \quad (4.14)$$

that implies $u_h > 0$ and $u_c = 0$. Conversely, if we use also the cooling¹ $u_c > 0$ that implies $T_{\text{sa}} < T_{\text{ai}}$. This means that we are looking for a way to know from our optimization problem if we need to cool or heat the room, and then eventually to know if we need to actuate against T_{sa} with the cooling system. In fact the inputs u_h and u_c , multiplied by c_{pa} , model respectively the portion of the ventilation heat flow due to heating and cooling.

¹We recall that in order to cool we actually need the ventilation system to be on.

Hence, the room temperature dynamics can be described by the LTI system

$$\begin{aligned} \dot{x}(k) &= A_c x(k) + B_c u(k) + E_c w(k) \\ y(k) &= C_c x(k), \end{aligned} \quad (4.15)$$

where $A_c = [a_{i,j}] \in \mathbb{R}^{13 \times 13}$ with

$$\begin{aligned} a_{1,1} &= h_i \frac{A_{\text{wall}}^1 + A_{\text{wall}}^2 + A_{\text{wall}}^3 + A_{\text{wall}}^4 + A_{\text{wall}}^5 + A_{\text{wall}}^6}{m_{\text{air}} c_{\text{pa}}} - \frac{1}{R_{\text{win}} m_{\text{air}} c_{\text{pa}}} \\ a_{1,2} &= 0 \\ a_{1,3} &= h_i \frac{A_{\text{wall}}^1}{m_{\text{air}} c_{\text{pa}}} \\ &\vdots \\ a_{1,12} &= 0 \\ a_{1,13} &= h_i \frac{A_{\text{wall}}^6}{m_{\text{air}} c_{\text{pa}}} \end{aligned}$$

$$\begin{aligned} a_{2,1} &= 0 \\ a_{2,2} &= -\frac{h_o A_{\text{wall}}^1}{C_{\text{wall}}^1} - \frac{1}{R_{\text{wall}}^1 C_{\text{wall}}^1} \\ a_{2,3} &= \frac{1}{R_{\text{wall}}^1 C_{\text{wall}}^1} \\ a_{2,4} &= 0 \\ &\vdots \\ a_{2,13} &= 0 \end{aligned}$$

$$\begin{aligned} a_{3,1} &= \frac{h_i A_{\text{wall}}^1}{C_{\text{wall}}^1} \\ a_{3,2} &= \frac{1}{R_{\text{wall}}^1 C_{\text{wall}}^1} \\ a_{3,3} &= -\frac{h_i A_{\text{wall}}^1}{C_{\text{wall}}^1} - \frac{1}{R_{\text{wall}}^1 C_{\text{wall}}^1} \\ a_{3,4} &= 0 \\ &\vdots \\ a_{3,13} &= 0 \\ &\vdots \\ a_{13,13} &= -\frac{h_i A_{\text{wall}}^6}{C_{\text{wall}}^6} - \frac{1}{R_{\text{wall}}^6 C_{\text{wall}}^6}, \end{aligned}$$

B_c and $E_c \in \mathbb{R}^{13 \times 3}$ equal to

$$B_c = \begin{bmatrix} \frac{1}{m_{air}} & \frac{1}{m_{air}} & \frac{A_{rad} h_{rad}}{m_{air} c_{pa}} \\ 0 & 0 & 0 \\ \vdots & \vdots & \vdots \\ 0 & 0 & 0 \end{bmatrix} \quad \text{and} \quad E_c = \begin{bmatrix} \frac{1}{R_{win} m_{air} c_{pa}} & \frac{G^1 * A_{win}^1}{m_{air}} & \frac{c}{m_{air} c_{pa}} \\ \frac{h_o A_{wall}^1}{C_{wall}^1} & \frac{h_o A_{wall}^1 \frac{a}{\alpha_e}}{C_{wall}^1} & 0 \\ 0 & 0 & 0 \\ \vdots & \vdots & \vdots \\ 0 & 0 & 0 \end{bmatrix},$$

$x(k) \in \mathbb{R}^{13}$ is the state vector containing the room temperature and the inner and outer temperatures of all the walls,

$$x(k) = \left[T_{room} \quad T_{wall,o}^1 \quad T_{wall,i}^1 \quad \dots \quad T_{wall,o}^6 \quad T_{wall,i}^6 \right]^\top$$

$u(k)$ and $w(k) \in \mathbb{R}^3$ are the vector of our inputs and the vector of random disturbances at time k respectively

$$u(k) = \left[u_h(k) \quad u_c(k) \quad \Delta T_{h,rad}(k) \right]^\top,$$

$$w(k) = \left[T_{amb}(k) \quad I^1(k) \quad N_{people}(k) \right]^\top$$

Since we want the room temperature at time k as our system output, our $C \in \mathbb{R}^{13}$ will be

$$C_c = \left[1 \quad 0 \quad \dots \quad 0 \right]$$

This continuous system is then discretized using the Backward Euler Method with a sampling time of 10'. This leads to the discrete LTI system

$$\begin{aligned} x(k+1) &= Ax(k) + Bu(k) + Ew(k) \\ y(k) &= Cx(k). \end{aligned} \tag{4.16}$$

The MPC problem for the room temperature can eventually be formulated as

Problem 4 (Formulation of the MPC for the room temperature).

$$\begin{aligned}
 \min_U \quad & \sum_{k=t}^{t+N-1} \begin{bmatrix} c_h & c_c & c_r \end{bmatrix} \begin{bmatrix} u_h(k) \\ u_c(k) \\ \Delta T_{h,\text{rad}}(k) \end{bmatrix} \\
 \text{subject to} \quad & \underline{u}_h \leq c_{\text{pa}} u_h(k) \leq \overline{u}_h & k = t, \dots, t + N - 1 \\
 & \underline{u}_c \leq c_{\text{pa}} u_c(k) \leq \overline{u}_c & k = t, \dots, t + N - 1 \\
 & \underline{u}_r \leq A_{\text{rad}} h_{\text{rad}} \Delta T_{h,\text{rad}}(k) \leq \overline{u}_r & k = t, \dots, t + N - 1 \\
 & \underline{y} \leq y(k) \leq \overline{y} & k = t, \dots, t + N - 1
 \end{aligned}$$

where

$$c_h = c_c = c_{\text{pa}}$$

$$c_r = A_{\text{rad}} h_{\text{rad}}$$

$$\underline{u}_h = 0$$

$$\overline{u}_h = c_{\text{pa}} \dot{m}_{\text{air}}^{\max} (T_{\text{ai}}^{\text{worst case}} - T_{\text{room}}^{\text{worst case}})$$

$$\underline{u}_c = 0$$

$$\overline{u}_c = c_{\text{pa}} \dot{m}_{\text{air}}^{\max} (T_{\text{ai}}^{\text{worst case}} - T_{\text{room}}^{\text{worst case}})$$

$$\underline{u}_r = 0$$

$$\overline{u}_r = A_{\text{rad}} h_{\text{rad}} \Delta T_{h,\text{rad}}^{\text{worst case}}$$

$$\underline{y} = y_{\min} = T_{\min}$$

$$\overline{y} = y_{\max} = T_{\max}$$

and only for the first sample t of the control horizon we add also

$$\underline{u}_h(t) = \underline{u}_h^* = c_{\text{pa}} \dot{m}_{\text{air}}^{\min} (T_{\text{ai}}(t) - T_{\text{room}}(t))$$

$$\underline{u}_c(t) = \underline{u}_c^* = c_{\text{pa}} \dot{m}_{\text{air}}^{\min} (T_{\text{ai}}(t) - T_{\text{room}}(t))$$

to take in account the minimal air flow needed $\dot{m}_{\text{air}}^{\min}$ calculated in (4.13)

Let x_0 denote the current state. It then follows from the linear model (4.16), that the room temperature dynamics over the prediction horizon N can be

written as

$$x(k) = A^k x_0 + \sum_{i=0}^{k-1} A^{k-i-1} B u(i) + \sum_{i=0}^{k-1} A^{k-i-1} E w(i).$$

Let then

$$\mathbf{Y} := [y_0^T, \dots, y_{N-1}^T]^T, \quad \mathbf{Y} \in \mathbb{R}^N \quad (4.17)$$

$$\mathbf{U} := [u_0^T, \dots, u_{N-1}^T]^T, \quad \mathbf{U} \in \mathbb{R}^{3N} \quad (4.18)$$

$$\mathbf{W} := [w_0^T, \dots, w_{N-1}^T]^T, \quad \mathbf{W} \in \mathbb{R}^{3N} \quad (4.19)$$

$$\mathbf{A} := \begin{bmatrix} (A)^T & \dots & (A^N)^T \end{bmatrix}^T \quad (4.20)$$

$$\mathbf{B} := \begin{bmatrix} B & \dots & \mathbf{0} \\ \vdots & \ddots & \\ A^{N-1}B & \dots & B \end{bmatrix} \quad (4.21)$$

$$\mathbf{E} := \begin{bmatrix} E & \dots & \mathbf{0} \\ \vdots & \ddots & \\ A^{N-1}E & \dots & E \end{bmatrix} \quad (4.22)$$

$$\mathbf{C} := \text{diag}(C, \dots, C) \quad (4.23)$$

$$\mathbf{G}_x := [\mathbf{C}\mathbf{A}] \quad (4.24)$$

$$\mathbf{G}_u := [\mathbf{C}\mathbf{B}] \quad (4.25)$$

$$\mathbf{G}_w := [\mathbf{C}\mathbf{E}] \quad (4.26)$$

$$\tilde{\mathbf{g}} := [-y_{\min}(k)^T \dots - y_{\min}(k)^T y_{\max}(k)^T \dots y_{\max}(k)^T]^T \quad (4.27)$$

$$\mathbf{g} := \tilde{\mathbf{g}} - \mathbf{G}_x x_0 \quad (4.28)$$

$$\mathbf{F} := \begin{bmatrix} -\mathbb{I}_{3N} \\ \mathbb{I}_{3N} \end{bmatrix} \quad (4.29)$$

$$\mathbf{f} := [-u_{\min}^T \dots - u_{\min}^T u_{\max}^T \dots u_{\max}^T]^T \quad (4.30)$$

$$\mathbf{H} := \begin{bmatrix} -1 & 0 & 0 & \dots & 0 \\ 0 & -1 & 0 & \dots & 0 \end{bmatrix} \quad (4.31)$$

$$\mathbf{h} := [-\underline{u}_h^* \quad -\underline{u}_c^*]^T \quad (4.32)$$

where $\mathbf{0}$ is a zero matrix with appropriate dimensions and $\mathbb{I}_{3N} \in \mathbb{R}^{3N \times 3N}$ is the identity matrix. Hence we can express the output \mathbf{Y} over the whole prediction

horizon, given the initial state x_0 , as

$$\mathbf{Y} = \mathbf{C}(\mathbf{A}x_0 + \mathbf{B}\mathbf{U} + \mathbf{E}\mathbf{W}) \quad (4.33)$$

and the constraints on the output and the inputs over the whole prediction horizon N as

$$\begin{aligned} \mathbf{G}_u\mathbf{U} + \mathbf{G}_w\mathbf{W} &\leq \mathbf{g} \\ \mathbf{F}\mathbf{U} &\leq \mathbf{f} \\ \mathbf{H}\mathbf{U} &\leq \mathbf{h}. \end{aligned}$$

Notice that we consider time varying bounds on the room temperature, $y_{\min}(k)$ and $y_{\max}(k)$, which accounts for the effects of time varying occupancy. For instance we can set different bounds for the day and for the night. We notice that it may be dangerous to have sets of bounds that differ very much. E.g., allowing really low temperatures during night periods may lead to severe power consumptions when the system has to raise the temperature when the day comes.

Post processing

The values obtained from the previous MPC problems can not be directly used to command the actuators. Indeed the assumptions made in Section 4.2, stating that the problems can be reduced to linear optimization problems, must be modified to account for the peculiarities of the hardware in the testbed. Our choice is to exploit a post-processing phase that transforms the information coming from the two previous MPCs into signals that correspond to how much the various valves of the plant should be open.

Consider then that the information coming from the temperature MPC is composed by u_c , u_h , ΔT_{mr} . From the CO₂ MPC instead provides \dot{m}_{air}^{\min} , the lower bound on the air flow rate. The following Algorithm 1 reports this transformation procedure. Notice that this algorithm does not handle T_{mr} because our tests have been performed during the summer season, where, as already said before, radiators do not receive warm water. We now comment Algorithm 1. The first three rows check if there is a simultaneous need of cooling and venting. This case is due with a big probability to the need of a ventilation carried by the last two constraints added in the Problem 4. If $u_c > u_h$ what

Algorithm 1 Post-processing

```

1: if  $u_h \geq 0$  and  $u_c \geq 0$  then
2:   if  $u_c \geq u_h$  then
3:      $u_c = u_c - u_h$ 
4: if  $u_h = 0$  and  $u_c = 0$  then
5:    $T_{sa} = 20.5$ 
6:    $\dot{m}_{air} = 0$ 
7: else if  $u_h \geq 0$  and  $u_c = 0$  then
8:    $T_{sa} = 20.5$ 
9:    $\dot{m}_{air} = \frac{u_h}{T_{ai} - T_{room}}$ 
10: else if  $u_c \geq 0$  then
11:   if  $\dot{m}_{air}^{\min} = 0$  then
12:      $T_{sa} = 16.5$ 
13:      $\dot{m}_{air} = \frac{u_h}{T_{room} - 0.7T_{ai} - 0.3T_{sa}}$ 
14:   else
15:      $\dot{m}_{air} = \dot{m}_{air}^{\min}$ 
16:      $T_{sa} = \frac{10}{3} \left( T_{room} - \frac{u_c}{\dot{m}_{air}} - 0.7T_{ai} \right)$ 
17:   if  $T_{sa} \leq 16.5$  then
18:      $T_{sa} = 16.5$ 
19:      $\dot{m}_{air} = \frac{u_h}{T_{room} - 0.7T_{ai} - 0.3T_{sa}}$ 
20:   else if  $T_{sa} \geq 20.5$  then
21:      $T_{sa} = 20.5$ 
22:      $\dot{m}_{air} = \frac{u_h}{T_{room} - 0.7T_{ai} - 0.3T_{sa}}$ 
23: if  $\dot{m}_{air} \leq \dot{m}_{air}^{\min}$  then
24:    $\dot{m}_{air} = \dot{m}_{air}^{\min}$ 

```

actually we have to do is to cool $u_c - u_h$. The opposite situation is managed from the row 10. From row 4 to 6 we are setting instead the parameters in order not to actuate anything. In fact the temperature of the cooling supply air is in average between 16.5°C the lowest temperature we saw from several measurements, and 20.5°C, the average temperature of the air inlet flow. From the row 7 to 9 we are facing the need of ventilation. That could be for heating purposes, fresh air purposes or also, accordingly with the temperature of the room, also for cooling purposes. If there is no need of cooling, it means that all the u_v will be translated to \dot{m}_{air} from the reverse formulation of (4.14). From the row 10 we are checking the need of cooling. The first step is to check the lower bound of the CO₂ model. If it is 0 we cool at the lowest temperature, trying to minimize the air mass flow². The formula in the row 13 come from the knowledge exposed in the Subsection 3.2 of a kind of average ratio of $3 \div 7$ between the cooling air flow (\dot{m}_{cool}) and the venting air flow³ (\dot{m}_{vent}). We can in fact think at the u_c as

$$u_c = \dot{m}_{\text{air}}(T_{\text{room}} - T_{\text{air}}) = \dot{m}_{\text{air}}(T_{\text{room}} - 0.7T_{\text{ai}} - 0.3T_{\text{sa}}), \quad (4.34)$$

considering T_{air} like a mixture of air form the two different branches. From the equation (4.34) are coming also the formulas in the rows 19 and 22, used to bound eventually cases where the formula in the row 13 takes us to lower or higher values of T_{sa} , that are set in the limits of our comfort range.

At the end we do a security check to be sure that the value that actually we are giving it is greater than the required lower bound. If at the end we have an \dot{m}_{air} different from 0[kg/s] it means that we have to actuate the corresponding percentage for the venting valve. Viceversa, if we have a T_{sa} that is lower than 20°C it means that we have to cool the room.

Transformation of the commands given by the CO₂ and temperature MPC into valves openings signals

The outcomes given by the previously described MPCs must be transformed into values for

1. $\Delta T_{h,\text{rad}}$, i.e., how much the valve relative to the radiators should be open;

²This is due to follow our assumption of a lower cost for the cooling action compared to the venting action

³The part that is coming only from the venting branch

2. \dot{m}_{vent} , i.e., how much the valve relative to the air venting should be open;
3. T_{sa} , i.e., how much the valve relative to the air cooling system should be open.

We now describe how we performed these transformations.

Mean radiant temperature $\Delta T_{h,\text{rad}}$ actually we do not threat this variable. As written in Section 3.2, our knowledge about this system is currently limited, and the system has been off during our experimental campaign so that identification procedures were not plausible.

Air mass flow \dot{m}_{vent} as written in Section 3.2 we model the relation between the needed air mass flow and the venting opening valve percentage as a linear relation. This implies that the transformation is a mere rescaling of the output of equation (3.21).

Temperature of the air conditioning supply air T_{sa} we devise two different possibilities, both based on the identified relation (3.22) in page 44. Both the solutions are based on an opportune space state model and the following assumption: during the time interval between two cycles of the MPCs,

- the venting valve opening percentage is constant ($A_v(t) = A_v$);
- $T_{\text{ai}}(t)$ is known and constant.

The first approach builds then the space-state system

$$\begin{aligned} \begin{bmatrix} x(k+1) \\ x_r(k+1) \end{bmatrix} &= \begin{bmatrix} \alpha & \beta \\ 1 & 0 \end{bmatrix} \begin{bmatrix} x(k) \\ x_r(k) \end{bmatrix} + \begin{bmatrix} \gamma A_v + \delta \\ 0 \end{bmatrix} u(k) + \begin{bmatrix} \epsilon T_{\text{ai}} \\ 0 \end{bmatrix} \\ y(k) &= \begin{bmatrix} 1 & 0 \end{bmatrix} \begin{bmatrix} x(k) \\ x_r(k) \end{bmatrix} \end{aligned} \quad (4.35)$$

where

$$\begin{aligned} x(k) &= T_{\text{sa}}(k) \\ x_r(k) &= x(k-1) = T_{\text{sa}}(k-1) \\ u(k) &= A_c(k) \quad (\text{cooling opening valve percentage}) \end{aligned} \quad (4.36)$$

At this point system (4.35) can be written as

$$\begin{aligned} \begin{bmatrix} x(k+1) \\ x_r(k+1) \end{bmatrix} &= A \begin{bmatrix} x(k) \\ x_r(k) \end{bmatrix} + Bu(k) + E \\ y(k) &= C \begin{bmatrix} x(k) \\ x_r(k) \end{bmatrix} \end{aligned} \quad (4.37)$$

Considering the constant input U_{reg} that carries the system to the equilibrium point $\bar{x} = T_{\text{sa,ref}}$ we find

$$x(k+1) = \bar{x} = A\bar{x} + BU_{\text{reg}} + E. \quad (4.38)$$

Solving the previous equation gives

$$U_{\text{reg}} = (B^\top B)B^\top [(I - A)\bar{x} - E] \quad (4.39)$$

It can be noticed that this kind of control law does not rely on feedback mechanisms.

The second solution is instead developed as follows: start from (4.35), and consider that we have a system with a constant disturbance on the state (the constant matrix E). Let then the input be $\Delta u(k)$ rather than $u(k)$. Adding the state

$$x_u(k) = u(k-1) \quad (4.40)$$

the whole system becomes

$$\begin{aligned} \begin{bmatrix} x(k+1) \\ x_r(k+1) \\ x_u(k+1) \end{bmatrix} &= \begin{bmatrix} \alpha & \beta & \gamma A_v + \delta \\ 1 & 0 & 0 \\ 0 & 0 & 1 \end{bmatrix} \begin{bmatrix} x(k) \\ x_r(k) \\ x_e(k) \end{bmatrix} + \begin{bmatrix} \gamma A_v + \delta \\ 0 \\ 1 \end{bmatrix} \Delta u(k) + \begin{bmatrix} \epsilon T_{\text{ai}} \\ 0 \\ 0 \end{bmatrix} \\ y(k) &= \begin{bmatrix} 1 & 0 & 0 \end{bmatrix} \begin{bmatrix} x(k) \\ x_r(k) \\ x_e(k) \end{bmatrix} \end{aligned} \quad (4.41)$$

that can also written as

$$\begin{aligned} \begin{bmatrix} x(k+1) \\ x_r(k+1) \\ x_u(k+1) \end{bmatrix} &= A \begin{bmatrix} x(k) \\ x_r(k) \\ x_u(k) \end{bmatrix} + B\Delta u(k) + E \\ y(k) &= C \begin{bmatrix} x(k) \\ x_r(k) \\ x_u(k) \end{bmatrix}. \end{aligned} \quad (4.42)$$

The optimal input can then be found as the solution of the following optimization problem:

Problem 5 (Formulation of the MPC for the control of the cooling actuation).

$$\begin{aligned} \min_{\Delta u(t), \dots, \Delta u(t+N-1)} \quad & \sum_{k=t}^{t+N-1} \left\| W^y [y(k+1) - r^*] \right\|^2 + \left\| W^{\Delta u} \Delta u(k) \right\|^2 \\ \text{subject to} \quad & \underline{u} \leq u(k) \leq \bar{u} \quad k = t, \dots, t+N-1 \\ & \underline{\Delta u} \leq \Delta u(k) \leq \overline{\Delta u} \quad k = t, \dots, t+N-1 \\ & \underline{y} \leq y(k) \leq \bar{y} \quad k = t, \dots, t+N-1 \end{aligned} \quad (4.43)$$

The constraint on $u(t)$, $\Delta u(t)$, $y(t)$ can be expressed as:

$$\begin{aligned} \mathcal{H}_A x_t + \mathcal{H}_B \Delta U + \mathcal{H}_E \mathbf{1}_{N \times 1} &\leq \bar{u} \mathbf{1}_{N \times 1} \\ \mathcal{H}_A x_t + \mathcal{H}_B \Delta U + \mathcal{H}_E \mathbf{1}_{N \times 1} &\geq \underline{u} \mathbf{1}_{N \times 1} \\ \mathbb{I} \Delta U &\leq \overline{\Delta u} \mathbf{1}_{N \times 1} \\ \mathbb{I} \Delta U &\geq \underline{\Delta u} \mathbf{1}_{N \times 1} \\ \mathcal{C}_A x_t + \mathcal{C}_B \Delta U + \mathcal{C}_E \mathbf{1}_{N \times 1} &\leq \bar{y} \mathbf{1}_{N \times 1} \\ \mathcal{C}_A x_t + \mathcal{C}_B \Delta U + \mathcal{C}_E \mathbf{1}_{N \times 1} &\geq \underline{y} \mathbf{1}_{N \times 1} \end{aligned} \quad (4.44)$$

where the involved matrices are

$$\begin{aligned}
 \mathcal{H}_A &= \begin{bmatrix} HA \\ HA^2 \\ \vdots \\ HA^N \end{bmatrix}, & \mathcal{H}_B &= \begin{bmatrix} HB & 0 & \dots & 0 \\ HAB & HB & & 0 \\ \vdots & & \ddots & \\ HA^{N-1}B & \dots & & HB \end{bmatrix}, & \mathcal{H}_E &= \begin{bmatrix} HE & 0 & \dots & 0 \\ HAE & HE & & 0 \\ \vdots & & \ddots & \\ HA^{N-1}E & \dots & & HE \end{bmatrix}, \\
 \mathcal{C}_A &= \begin{bmatrix} CA \\ CA^2 \\ \vdots \\ CA^N \end{bmatrix}, & \mathcal{C}_B &= \begin{bmatrix} CB & 0 & \dots & 0 \\ CAB & CB & & 0 \\ \vdots & & \ddots & \\ CA^{N-1}B & \dots & & CB \end{bmatrix}, & \mathcal{C}_E &= \begin{bmatrix} CE & 0 & \dots & 0 \\ CAE & CE & & 0 \\ \vdots & & \ddots & \\ CA^{N-1}E & \dots & & CE \end{bmatrix}, \\
 H &= \begin{bmatrix} 0 & 0 & 1 \end{bmatrix}, & x_t &= \begin{bmatrix} x(t) \\ x_r(t) \\ x_u(t) \end{bmatrix} = \begin{bmatrix} T_{sa}(t) \\ T_{sa}(t-1) \\ A_c(t) \end{bmatrix}, & \Delta U &= \begin{bmatrix} \Delta u(t) \\ \Delta u(t+1) \\ \vdots \\ \Delta u(t+N-1) \end{bmatrix}.
 \end{aligned}$$

The cost function minimization problem in (4.43), taking the weight matrices equal to

$$W^y = \mathbb{I}_{N \times N}, \quad W^{\Delta u} = \theta \mathbb{I}_{N \times N}$$

becomes

$$\begin{aligned}
 & \min_{\Delta U} \sum_{k=t}^{t+N-1} [y(k+1) - r^*]^\top [y(k+1) - r^*] + \theta \sum_{k=t}^{t+N-1} \Delta u(k)^2 \\
 &= \min_{\Delta U} 2x_t^\top \mathcal{C}_A^\top \mathcal{C}_B \Delta U + 2(\mathcal{C}_E \mathbf{1} - r^* \mathbf{1})^\top \mathcal{C}_B + \Delta U^\top \mathcal{C}_B^\top \mathcal{C}_B \Delta U + \Delta U^\top \Delta U \\
 &= \min_{\Delta U} \underbrace{2[x_t^\top \mathcal{C}_A^\top + (\mathcal{C}_E \mathbf{1} - r^* \mathbf{1})^\top] \mathcal{C}_B}_{\Omega} \Delta U + \Delta U^\top \underbrace{[\mathcal{C}_B^\top \mathcal{C}_B + \theta \mathbb{I}_{N \times N}]}_{\Phi} \Delta U
 \end{aligned} \tag{4.45}$$

and where r^* is the reference signal, constant during the whole control horizon. The whole problem can be written as:

$$\begin{aligned}
 & \min_{\Delta U} \quad \Omega \Delta U + \Delta U^\top \Phi \Delta U \\
 & \text{subject to} \quad \mathbf{G} \Delta U \leq \mathbf{S} x_t + \mathbf{W}
 \end{aligned}$$

where \mathbf{G} , \mathbf{S} and \mathbf{W} are built accordingly with (4.44).

5

Experimental Results

5.1 Testing the MPC solution adopted to control the cooling actuation

Before testing the whole MPC strategy we tested the second level controller presented in Section 4.2 at page 67. This controller receives from the main MPC a constant venting percentage and a reference T_{sa} and then aims to carry the system to that reference in less than two MPC sampling periods (10 seconds in our case). We notice that we do not explore the numerous different situations that the system may face, and present only a subset of the meaningful cases.

The first numerical example simulates an active ventilation with set point at 30% and two different temperature references: 17°C and 18°C. In both the cases the initial condition is set to 20°C. Results plotted in Figure 5.1 and 5.2 indicate the validity of the proposed controller, since it reaches the reference signal in both cases in less than 8' without any error.

Before testing the whole MPC scheme we then check how the first proposed implementation works on real systems. The following Figures 5.3 and 5.4 show that with a reference signal of 17°C the T_{sa} perfectly reaches the target

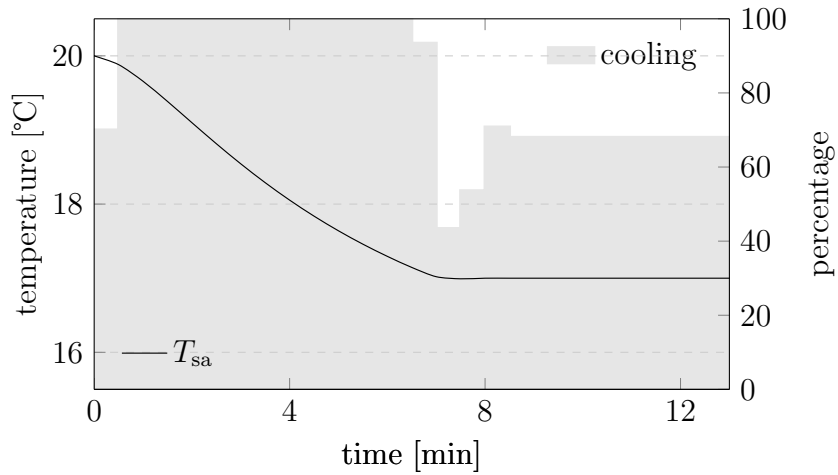


Figure 5.1: Simulation on the second level MPC for the T_{sa} . The reference is set to 17°C the ventilation is constant at 30%.

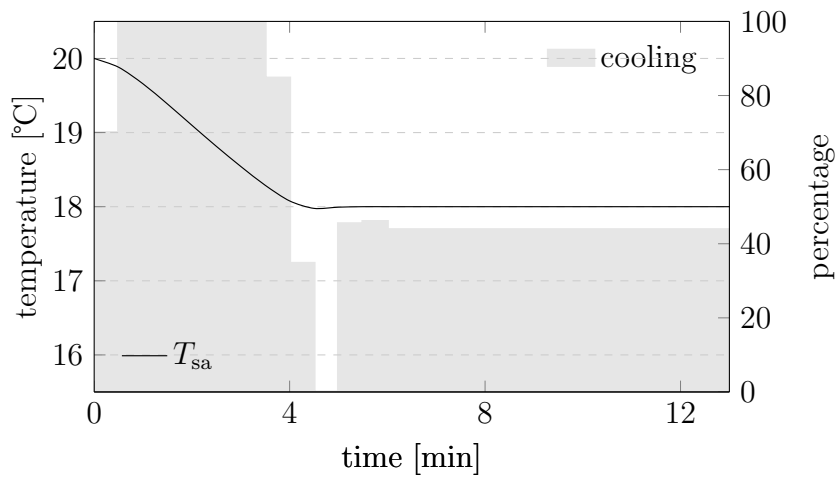


Figure 5.2: Simulation on the second level MPC for the T_{sa} . The reference is set to 18°C the ventilation is constant at 30%.

(Figure 5.3). But when the reference changes to 18°C, then T_{sa} struggles to cross the 19°C threshold (Figure 5.4) with around one degree of error. This error is not tolerable for our purposes.

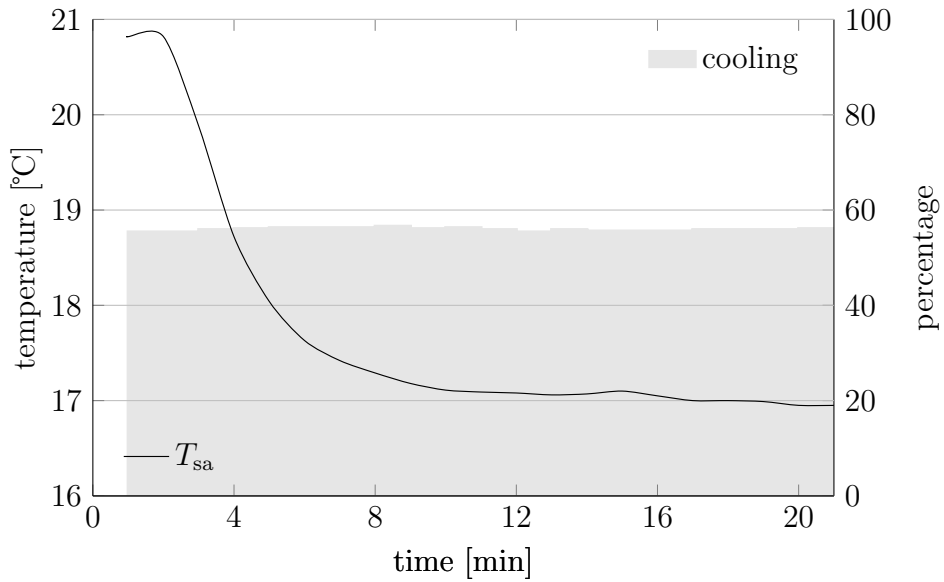


Figure 5.3: Test on the equilibrium point method for the T_{sa} . The reference is set to 17°C and the ventilation is constant at 30%.

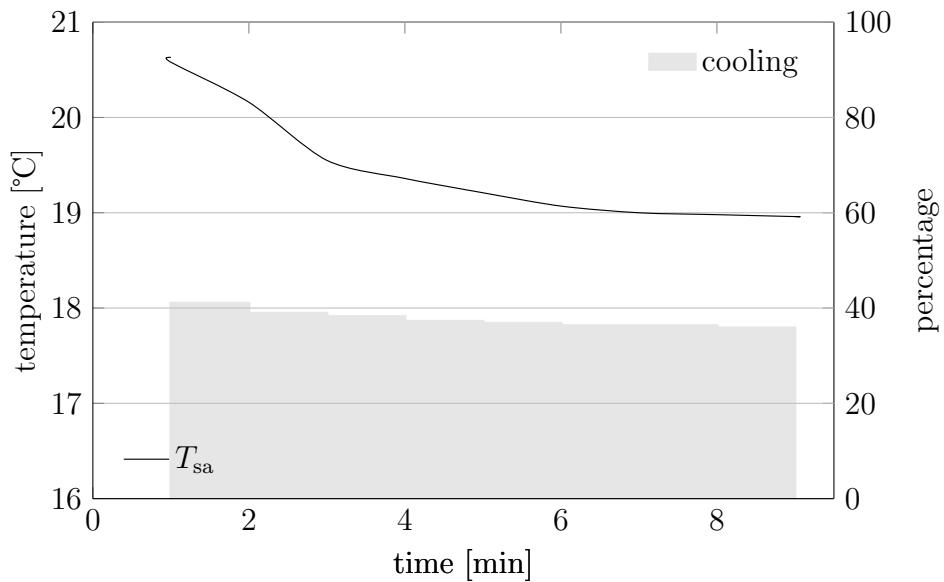


Figure 5.4: Test on the equilibrium point method for the T_{sa} . The reference is set to 18°C and the ventilation is constant at 30%.

The results given instead applying the MPC controller to the real system are shown in Figure 5.5 and 5.6.

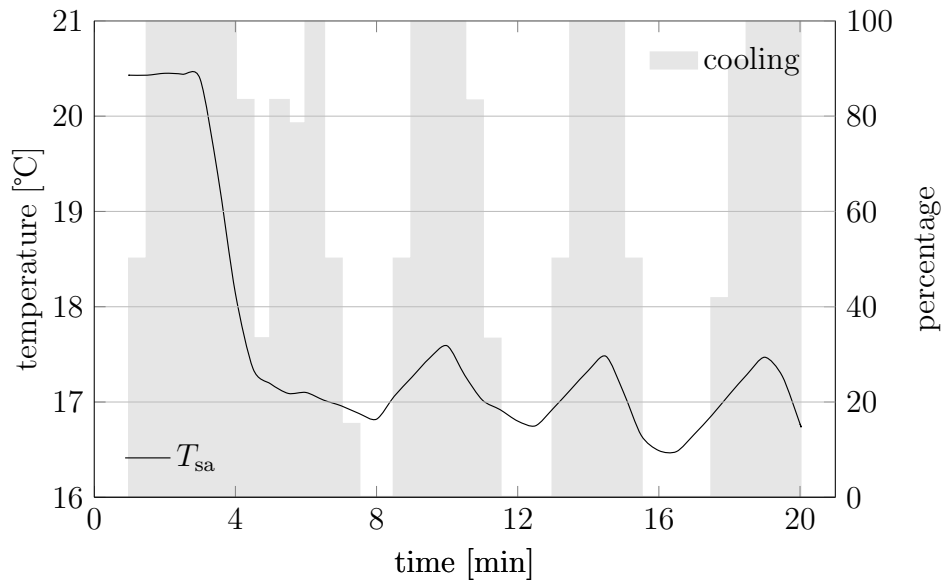


Figure 5.5: Test on the MPC for the T_{sa} . The reference is set to 17°C and the ventilation is constant at 30%.

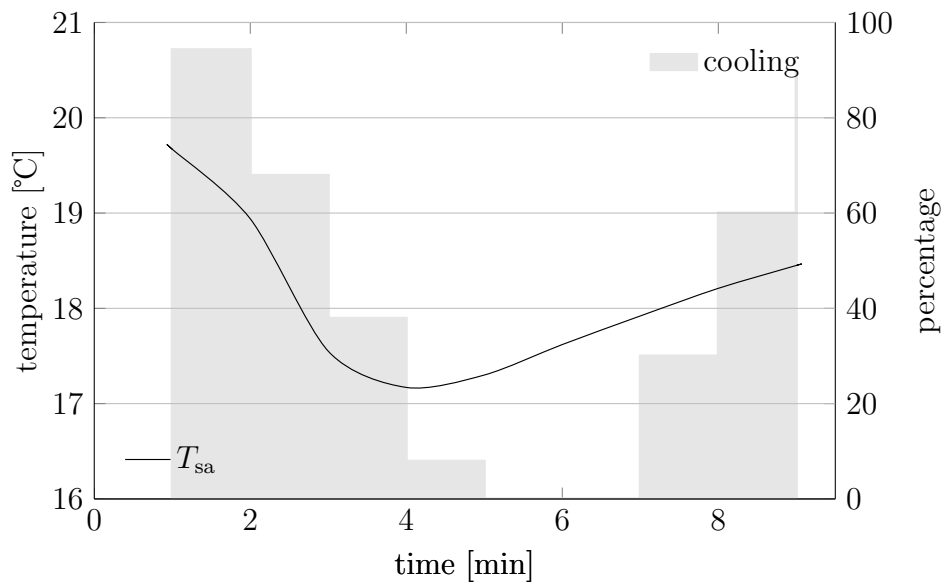


Figure 5.6: Test on the MPC for the T_{sa} . The reference is set to 18°C and the ventilation is constant at 30%.

We can notice that the equilibrium is never reached, and that there exists a swinging response around the reference temperature. Furthermore the required temperature is never precisely reached. The comparison between these controllers lead us to choose the second strategy to solve problem 5 because it seems more reliable and respecting the conditions of the system.

5.2 Test of the whole MPC

We now present the results that we obtained applying our controller to the testbed. To this aim we consider four separated tests.

We start describing how we selected the constraints more formally. As for the bounds of the input commands, in all the tests we set them according to some assumptions on the available power of our systems. We thus computed these bounds starting from the equations for Q_{vent} , Q_{cool} and Q_{heat} in (3.2) in page 30 and from (3.14) at page 35 for u_{CO_2} . We then choose to consider the worst initial conditions that our system could face, and thus computed the corresponding theoretically available power. For instance for the ventilation we have

$$\begin{aligned} \dot{m}_{\text{air}}^{\min} &= 0 & \dot{m}_{\text{air}}^{\min} &\approx 0.4 \\ T_{\text{ai}}^{\min} &\approx 20 & T_{\text{ai}}^{\max} &\approx 22 \\ T_{\text{room}}^{\min} &\approx 15 & T_{\text{room}}^{\max} &\approx 26. \end{aligned}$$

With this assumption it follows

$$\begin{aligned} Q_{\text{air}}^{\min} &= 0 \\ Q_{\text{air}}^{\max} &\approx c_{\text{pa}} \left[\frac{J}{KgK} \right] 0.4 \left[\frac{kg}{s} \right] \cdot 7K \approx 3kW < 3.5W. \end{aligned}$$

The bound thus corresponds to

$$\begin{aligned} Q_{\text{vent}}^{\min} &= 0 \\ Q_{\text{vent}}^{\max} &= 3.5kW \\ Q_{\text{cool}}^{\min} &= 0 \\ Q_{\text{cool}}^{\max} &= 3kW \\ Q_{\text{rad}}^{\min} &= 0 \\ Q_{\text{rad}}^{\max} &= 8kW \end{aligned}$$

To test the CO₂ MPC we used a slightly different approach, and set the bounds accordingly with the status of the system. More precisely we assume

that the $C_{\text{CO}_2,i}$ concentration is constant, equal to the external one and thus assumed to be 390 ppm. The bounds are thus set to

$$\begin{aligned} \dot{m}_{\text{air}}^{\min}(x_{\text{CO}_2}(k) - C_{\text{CO}_2,i}) &\leq u_{\text{CO}_2}(k) \leq \dot{m}_{\text{air}}^{\max}(x_{\text{CO}_2}(k) - C_{\text{CO}_2,i}) \\ 0 &\leq u_{\text{CO}_2}(k) \leq 0.4(x_{\text{CO}_2}(k) - 390). \end{aligned}$$

The bounds setting our comfort levels have then been derived using the configuration suggested by Akademiska Hus. I.e., we copied the settings for the controller described in Section 4.1 in page 49. The dead zone band adopted has thus been decided using a trade off between the wellness of the room occupants. Notice that we did not force a small set of plausible temperatures to our MPC solver: in this way we minimize risks of infeasible optimization problems.

In total we set up 4 tests:

- **Test 1:**

- Temperature bounded between 20 °C to 23 °C
- CO₂ bounded under 700 ppm
- Period: 3 hours, between 11am and 2pm

The results are shown in Figure 5.7 at page 80

- **Test 2:**

- Temperature bounded between 20 °C to 23 °C
- CO₂ bounded under 700 ppm
- Period: 1.5 hours, between 2:30pm and 4pm

The results are shown in Figure 5.8 at page 81

- **Test 3:**

- Temperature bounded between 20 °C to 23 °C
- CO₂ bounded under 700 ppm
- Period: 3 hours, between 10am and 1pm

The results are shown in Figure 5.9 at page 82

- **Test 4:**
 - Temperature bounded between 20 °C to 23 °C
 - CO₂ bounded under 750 ppm
 - Period: 1 hours, between 2pm and 3pm

The results are shown in Figure 5.9 at page 82

To run these tests we provide to our controller weather, thermal radiations and occupancy forecasts. To this point we set:

- **Weather forecasts:** a linear interpolation of the hourly web forecasts (described in Section 2.2 at page 24) accordingly with our sampling period and our prediction horizon;
- **Solar radiation forecasts:** the tested area is not exposed to solar radiation since it lies in the basements of the building. The windows are either never hit by the solar rays or too small to let the solar radiation influence significantly the comfort levels. Thereby we consider a null effect for the whole period;
- **Occupancy forecasts:** to predict the occupancy we decided to use the corresponding patterns of the very past week.

The proposed main MPC program runs every 10 minutes with a prediction horizon of 8 hours. The low level MPC, as anticipated in Section 4.2 at page 67 and whose results are shown in Section 5.1, works when the main MPC requires cooling actuation. From practical perspectives it works every minute for the ten minutes needed. Figures 5.7, 5.8, 5.9, and 5.10 present the results of our tests.

In all the tests the proposed control schemes respect almost everywhere the comfort bounds. We indeed notice that during these experiments the room temperature crossed the bound only few times and only for really short periods. In all the cases the output of the CO₂ MPC did not give to the temperature MPC any bound. Test 4 then considers a case where the room occupancy is

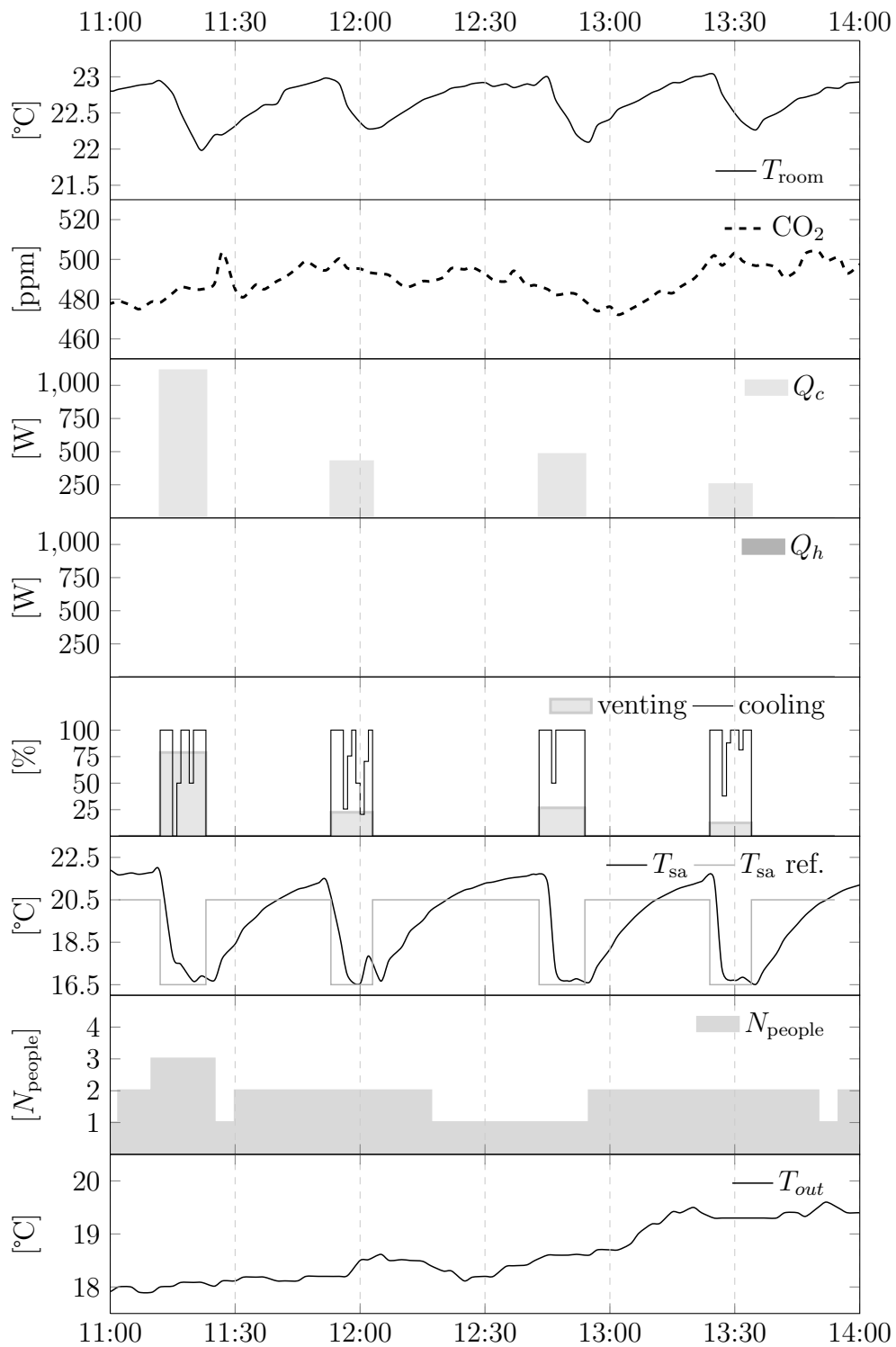


Figure 5.7: Test 1 on the MPC. The temperature comfort bounds are set to 20 $^{\circ}\text{C}$ to 23 $^{\circ}\text{C}$ while the upper bound of the CO₂ concentration is 700 ppm.

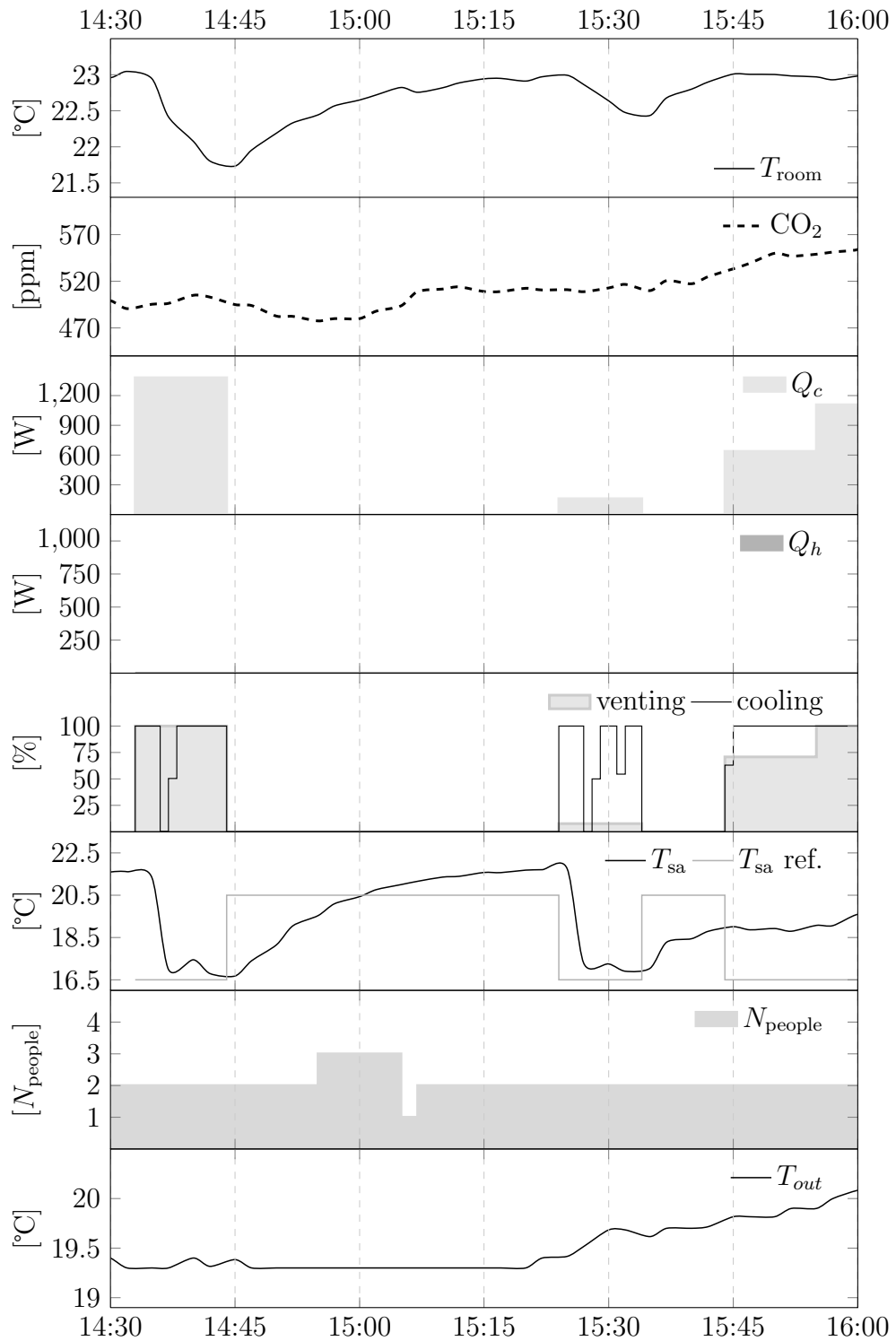


Figure 5.8: Test 2 on the MPC. The temperature comfort bounds are set to 20 $^{\circ}\text{C}$ to 23 $^{\circ}\text{C}$ while the upper bound of the CO₂ concentration is 700 ppm.

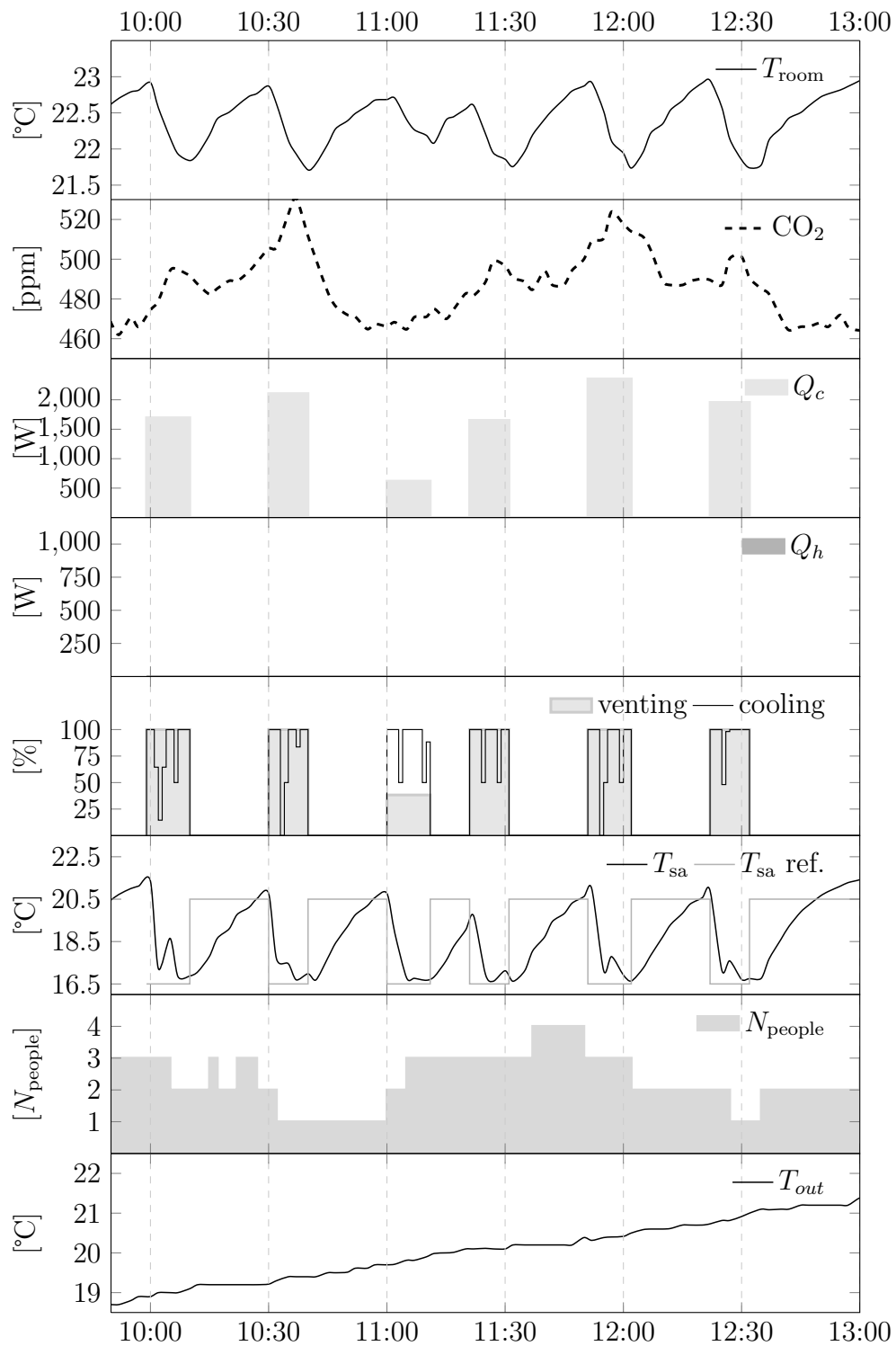


Figure 5.9: Test 3 on the MPC. The temperature comfort bounds are set to 20 $^{\circ}\text{C}$ to 23 $^{\circ}\text{C}$ while the upper bound of the CO₂ concentration is 700 ppm.

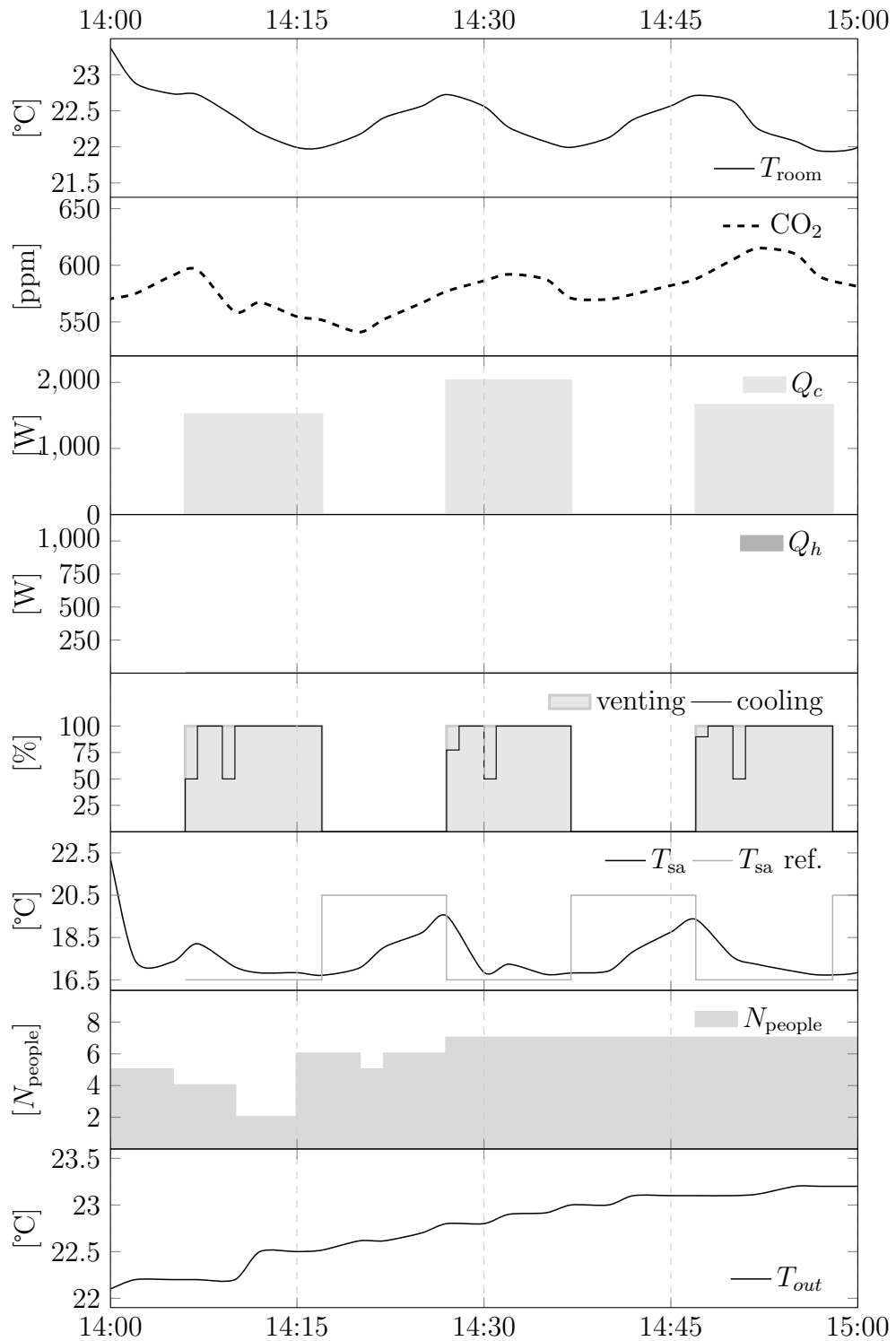


Figure 5.10: Test 4 on the MPC. The temperature comfort bounds are set to 20 $^{\circ}\text{C}$ to 23 $^{\circ}\text{C}$ while the upper bound of the CO₂ concentration is 750 ppm.

very high, meaning thus a high CO_2 production rate. Even in this case no lower bounds has been reached: first of all the CO_2 concentration never reached alert levels. This is also thanks to the Temperature MPC, that with its effort to decrease the temperature provided an additional boost to the ventilation system and thus helping the CO_2 to decrease.

We also notice that, as expected, during the tests the MPC controllers were not requiring heat demands. The cooling action performed by the low level MPC moreover reproduced our expectations, and the T_{sa} followed gracefully the given reference. Let us clarify that the temperatures referring to the periods for which the ventilation system was not active do not invalidate the heat balance. In fact in this case no air is flowing out of the cooling outlet and thus no cooling action is given to the environment.

Finally, to evaluate the goodness of our controller we should compare it with the current practice PI used by Akademiska Hus. We then notice that performing such a comparison is actually a very difficult task. Indeed different control systems are meaningfully comparable only when facing the same conditions. Even knowing exactly figures for the amounts of consumed powers would not ameliorate this issue. In any case since the PI just neglect considerations about energy efficiency while our MPC is actually tailored for that purpose, we make the rather intuitive claim that probably our controller is less energy-hungry. We also assert that our controller is, from rational points of view, showing a generally more meaningful behavior. Consider in fact the plotted behavior of the default controller in Figure 4.1 on page 50, and consider that the performance is often inefficient. Constraint violations are indeed very frequent and the high frequency of the actuation commands neglects actuators wear considerations. Our controller instead generates much smoother reference signals, and violates much fewer times the comfort bounds.

6

Conclusions

The experience we matured designing the controller tells us that a necessary condition to derive meaningful control laws is to be aware of how the actuators work. Designers must have precise knowledge on how the actuation commands are influencing the controlled system, otherwise actuation could actually lead to negative effects. Models and controllers must be derived and designed only after a deep understanding of the structure of the whole system.

An other lesson learned is that there is actually space for improving the energy efficiency of buildings by just acting on the control laws. Accordingly to some experts opinions, the building where the testbed is located is rather well insulated and with good actuation systems. Nevertheless our experiments suggest that its energy demand could be greatly diminished. In this regards, we notice that who is managing the system seems to be not so conscious of what the current control system is actually doing. In any case, the current practice is for sure not considering important information such as weather forecasts and occupancy models. Moreover the current control scheme is neglecting energy efficiency considerations. We thus feel like to claim that a more mindful approach to the control of the indoor conditions could give serious improvements both on the wealth of the occupants and on the energetic bills.

Even if we could not measure the actual energy consumption of the two schemes, we are confident that our method, if well designed, is better from many point of views. The main conclusion that we draw from the analysis of the results of the tests we performed is that predictions play a big role in obtaining meaningful control rules. We eventually report that we actually do not know if it is more important to have better occupancy predictions, better model accuracy or more consistent forecast predictions. This thesis in fact faced the general problems that raise when making the system run for the first time, and only scratched the surface of the mountain of problems and interesting hidden questions. Nonetheless it has signed a possible path, and shown that the path is meaningful and full of promises.

7

Further developments

At the end of this path we are conscious that this field could be rich of possible improvement and possible questions that only a deeper study could show. We present now a list of prospects that came out working on this thesis.

Improving the temperature model the physical model we used is built using parameters based on experience and knowledge of the building. Usually data catch from a data sheet or based on these assumption are far from the actual values. May be an identification on the parameters that are composing the matrix could be a way to understand more about the dynamics of the variables of the building.

Multi-zone controller it could be interesting to extend the controller we designed to a multi-zone area.

Performing a study on the role of the information the controller is catching a lot of data from the testbed but actually we do not know if all are useful for control purposes. A study that shows which data are meaningful and which data are not, should reduce the dimension of the system and the

computational control effort.

Identify a relation for the radiator actuation the test we did on the radiator was insufficient. Fortunately we have run tests on the summer time thus this actuation was useless. In winter time a better knowledge on this argument is fundamental to guarantee the wellness of the occupants, especially with the cold Swedish weather.

Forecasts the occupancy forecasts to date are given by the patterns of the previous week. An improvement of this prediction method could effect the controller performances. It should be interesting to test how much good predictions can change the MPC control strategy.

SMPC and Soft constraints it could be performed the implementation of different kind of MPC. For instance to avoid some infeasibility problems trying to squeeze the comfort bound band it should be interesting to implement soft constraint on the MPC problem formulation. Moreover the forecasts could be seen as stochastic variables and thus it could be interesting also to develop a Chance Constraint MPC.

Energy efficiency to date we are not aware about how much money our actuation costs. It should be interesting to find a direct relationship between the valve opening and the energetic bill.

Bibliography

- [1] T. A. Nguyen and M. Aiello, “Energy Intelligent Buildings based on User Activity: A Survey,” *Energy and Buildings*, 2012.
- [2] K. Padmanabh and A. Malikarjuna, “iSense: a Wireless Sensor Network based Conference Room Management System,” in *Proceedings of the First ACM Workshop on Embedded Sensing Systems for Energy-Efficiency in Buildings - BuildSys '09*, 2009, pp. 37–42.
- [3] A. Barbato, L. Borsani, A. Capone, and S. Melzi, “Home energy saving through a user profiling system based on wireless sensors,” *Proceedings of the First ACM Workshop on Embedded Sensing Systems for Energy-Efficiency in Buildings - BuildSys '09*, p. 49, 2009.
- [4] T. Nguyen and M. Aiello, “Beyond Indoor Presence Monitoring with Simple Sensors,” in *Proceedings of the 2nd International Conference on Pervasive and Embedded Computing and Communication Systems*, 2012.
- [5] J. Lu, T. Sookoor, V. Srinivasan, G. Gao, B. Holben, J. Stankovic, E. Field, and K. Whitehouse, “The Smart Thermostat : Using Occupancy Sensors to Save Energy in Homes,” in *Proceedings of the 8th ACM Conference on Embedded Networked Sensor Systems (SenSys'102)*, 2010.
- [6] Y. Agarwal, B. Balaji, R. Gupta, J. Lyles, M. Wei, and T. Weng, “Occupancy-driven energy management for smart building automation,” *Proceedings of the 2nd ACM Workshop on Embedded Sensing Systems for Energy-Efficiency in Building - BuildSys '10*, p. 1, 2010.
- [7] G. R. Newsham and B. J. Birt, “Building-level occupancy data to improve ARIMA-based electricity use forecasts,” *Proceedings of the 2nd ACM*

- Workshop on Embedded Sensing Systems for Energy-Efficiency in Building - BuildSys '10*, p. 13, 2010.
- [8] B. Dong, K. P. Lam, C. P. Neuman, U. Technologies, and E. Hartford, "Integrated Building Control based on Occupant Behaviour Pattern Detection and Local Weather Forecasting," in *Proceedings of Building Simulation 2011: 12th Conference of International Building Performance Simulation Association, Sydney, Australia*, vol. 3, 2011, pp. 14–16.
- [9] H. Hagrais, V. Callaghan, and E. Al., "Creating an Ambient-Intelligence Environment Using Embedded Agents," *IEEE*, vol. 19, no. 6, pp. 12–20, 2004.
- [10] S. Hay and A. Rice, "The Case for Apportionment," in *Proceedings of the First ACM Workshop on Embedded Sensing Systems for Energy-Efficiency in Buildings - BuildSys '092*, 2009, pp. 13–18.
- [11] V. L. Erickson, M. A. Carreira-perpi nán, and A. E. Cerpa, "OBSERVE : Occupancy-Based System for Efficient Reduction of HVAC Energy," in *Information Processing in Sensor Networks (IPSN), 10th International Conference*, 2011, pp. 258–269.
- [12] V. L. Erickson, Y. Lin, A. Kamthe, R. Brahme, A. Surana, A. E. Cerpa, M. D. Sohn, and S. Narayanan, "Energy efficient building environment control strategies using real-time occupancy measurements," in *BuildSys2009*, Nov. 2009, pp. 19–24.
- [13] P. Davidsson and M. Boman, "Distributed monitoring and control of office buildings by embedded agents," *Information Sciences*, vol. 171, no. 4, pp. 293–307, May 2005.
- [14] Z. N. Zhen, Q. S. Jia, C. Song, and X. Guan, "An Indoor Localization Algorithm for Lightning Control Using RFID," in *Energy 2030 Conference*, 2008, pp. 1–6.
- [15] Y. Kim, Z. Charbiwala, A. Singhanian, T. Schmid, and M. B. Srivastava, "SPOTLIGHT: Personal Natural Resource Consumption Profiler," in *HotEmNets 2008*, 2008.

- [16] R. K. Harle and A. Hopper, "The Potential for Location-Aware Power Management," in *Proceedings of the 10th International Conference on Ubiquitous Computing, UbiComp '08, ACM*, 2008, pp. 302–311.
- [17] L. Hawarah, S. Ploix, and E. Al., "User Behaviour Prediction in Energy Consumption in Housing Using Bayesian Networks," in *Proceedings of the 10th International Conference on Artificial Intelligence and Soft Computing*, 2010, pp. 372–379.
- [18] M. Mozer, "The Neural Network House: an Environment that Adapts to its Inhabitants," in *Proceedings of the American Association for Artificial Intelligent*.
- [19] R. H. Dodier, G. P. Henze, D. K. Tiller, and X. Guo, "Building occupancy detection through sensor belief networks," *Energy and Buildings*, vol. 38, no. 9, pp. 1033–1043, Sept. 2006.
- [20] W. Kastner, M. J. Kofler, and C. Reinisch, "Using AI to Realize Energy Efficient Yet Comfortable Smart Homes," in *Proceedings of 8th IEEE International Workshop on Factory Communication Systems (WFCS '10)*, 2010, pp. 169–172.
- [21] R. V. Andersen, B. Olsen, and J. Tftum, "Simulation of the effect of occupant behaviour on indoor climate and energy consumption," in *Proceedings of Cima 2007 WellBeing Indoors*, 2007.
- [22] D. Bourgeois, C. Reinhart, and I. Macdonad, "Adding advanced behaviour models in whole building energy simulation: A study on the total energy impact of manual and automated lighting control," *Energy and Buildings*, vol. 38, p. 814:813, 2006.
- [23] S. H. Cho and M. Zaheer-uddin, "Predictive Control of intermittently operated radiant floor heating system," *Energy and Conversion Management*, vol. 49, pp. 1333–1342, 2003.
- [24] W. J. Grunenfelder and J. Todtli, "The use of weather predictions and dynamic programming in the control of solar domestic hot water systems," in *Mediterranean Electrotechnical Conference of IEEE Region 8 Conference*, 1985.

- [25] M. Gwerder and J. Todtli, “Predictive control for integrated room automation,” in *8th REHVA World Congress for Building Technologies*, 2005.
- [26] G. P. Henze, D. E. Kalz, S. Liu, and C. Felssman, “Experimental analysis of model-based predictive optimal control for active and passive building thermal storage inventory,” *HVAC & RESEARCH*, vol. 11, no. 2, 2005.
- [27] “SIA Standard 382/1. Luftungs- und klimaanlagen - allgemeine grundlagen und anforderungen,” 2006.
- [28] “SIA Standard 380/4. Elektrische energie im Hochbau,” 2006.
- [29] A. E. D. Mady, G. M. Provan, C. Ryan, and K. N. Brown, “Stochastic Model Predictive Controller for the Integration of Building Use and Temperature Regulation,” in *Proceedings of the Twenty-Fifth AAAI Conference on Artificial Intelligence*, Aug. 2011.
- [30] Y. Ma and F. Borrelli, “Fast stochastic predictive control for building temperature regulation,” in *American Control Conference*, 2012, pp. 3075–3080.
- [31] F. Oldewurtel, A. Parisio, C. N. Jones, D. Gyalistras, M. Gwerder, V. Stauch, B. Lehmann, and M. Morari, “Use of model predictive control and weather forecasts for energy efficient building climate control,” *Energy and Buildings*, vol. 45, pp. 15–27, Feb. 2012.
- [32] A. Parisio, M. Molinari, D. Varagnolo, and K. H. Johansson, “A Scenario-based Predictive Control Approach to Building HVAC Management Systems,” in *IEEE Conference on Automation Science and Engineering*, 2013.
- [33] D. Sturzenegger, D. Gyalistras, M. Gwerder, C. Sagerschnig, M. Morari, and R. S. Smith, “Model Predictive Control of a Swiss office building,” in *Clima-RHEVA World Congress*, 2013.
- [34] Y. Ma, A. Kelman, A. Daly, and F. Borrelli, “Predictive Control for Energy Efficient Buildings with Thermal Storage,” *IEEE CONTROL SYSTEMS MAGAZINE*.
- [35] Irisys, “Irc3000,” in <http://www.irisys.co.uk/people-counting/irc3000>.
- [36] —, “Irc3030,” in <http://www.irisys.co.uk/people-counting/irc3030>.

-
- [37] Fidelix, “Fx-2025a,” in <http://www.irisys.co.uk/people-counting/irc3000>.
- [38] G. A. Johannesson, “Mdels parameters for the thermal performance of buildings,” Ph.D. dissertation, Lund Technical University, 1981.
- [39] E. S. A. 2002, “Ida indoor climate and energy,” in <http://www.equa-solutions.co.uk/en/software/idaice>.
- [40] L. Ljung, *System Identification: Theory for the User*. P T R Prentice Hall, 1987.
- [41] F. Borrelli, A. Bemporad, and M. Morari, “Predictive Control for Linear and Hybrid Systems,” 2011.
- [42] IBM, “Cplex optimizer,” in <http://www-01.ibm.com/software/commerce/optimization/cplex-optimizer/>.
- [43] C. R. Inc., “Cvx,” in <http://cvxr.com/cvx/>.
- [44] D. Gyalistras and M. Gwerder, “Use of weather and occupancy forecasts for optimal building climate control (OptiControl): Two years progress report,” . . . *Systems Ecology ETH Zurich, Switzerland and Building . . .*, no. September, 2010.